Efficient Biclique Counting in Large Bipartite Graphs

ABSTRACT

Given a bipartite graph $G(U, V, E)$, a biclique is a complete subgraph (X, Y) where $X \subseteq U, Y \subseteq V$ and every vertex $u \in X$ is connected to every vertex in $v \in Y$. A (p, q)-biclique is a biclique with $|X| = p, |Y| = q$. Counting (p, q)-bicliques in bipartite graphs is an important operator for many applications, such as densest subgraph detection, cohesive subgraph analysis, and information aggregation in graph neural networks. However, getting the count of (p, q)-bicliques for large p and q (e.g., $p, q \geq 10$) is extremely difficult, because the number of (p, q)-bicliques increases exponentially with respect to p and q. The state-of-the-art algorithm for this problem is based on the (p, q)-biclique enumeration technique which is often very costly for large p and q due to the exponential blowup in the enumeration space of large (p, q)-bicliques. To overcome this problem, we first propose a novel exact algorithm, called EPivoter, based on a newly-developed maximal biclique enumeration technique. The striking feature of EPivoter is that it can count (p, q)-bicliques for all p and q using a combinatorial technique, instead of exhaustively enumerating all (p, q)-bicliques. Second, we propose a novel dynamic programming (DP) based h-zigzag sampling technique to approximately count the (p, q)-bicliques, where a h-zigzag is a simple path in the (p, q)-biclique with length $2h - 1$ ($h = \min\{p, q\}$). We prove that our DP-based sampling algorithm not only consumes near-linear time using near-linear space, but it can also obtain unbiased estimators for the counts of the (p, q)-bicliques for all p and q. Third, to further improve the efficiency, we also propose a hybrid algorithm that integrates both the exact EPivoter algorithm and our sampling algorithm. The hybrid algorithm is based on a carefully-designed graph splitting strategy that partitions the bipartite graph into sparse and dense regions. Then, it applies EPivoter to the sparse regions and the sampling algorithm to the dense regions to compute the (p, q)-biclique counts. Extensive experiments on 14 real-world graphs demonstrate that our algorithms significantly outperform the state-of-the-art algorithm.

ACM Reference Format:

. 2022. Efficient Biclique Counting in Large Bipartite Graphs. In *Proceedings of ACM Conference (Conference'17).* ACM, New York, NY, USA, 21 pages. https://doi.org/10.1145/nnnnnnn.nnnnnnn

1 INTRODUCTION

Given a bipartite graph $G(U, V, E)$ which comprises two disjoint vertex sets U and V and an edge set $E \subseteq U \times V$. A (p, q)-biclique in G is a complete subgraph $C(L, R)$ of G with $|L| = p$, $|R| = q$, and $\forall (u, v) \in L \times R, (u, v) \in E$. In this paper, we focus on the problem of counting (p, q)-bicliques for every pairs of p and q. Counting the bicliques in a bipartite graph is a fundamental operator for many higher-order bipartite graph analysis applications. We give two concrete examples as follows.

Higher-order clustering coefficient. The higher-order clustering coefficient based on traditional k-clique [36, 37] is an important metric to analyze the statistical properties of complex networks. It was shown in [36] that networks from the same domain often have similar higher-order clustering coefficient characteristics. As indicated in [36, 37], such a higher-order clustering coefficient can be easily extended to bipartite graphs. Specifically, in bipartite graphs, the higher-order clustering coefficient can be defined as the ratio between the counts of (p, q)-bicliques and (p, q)-*wedges*, where a (p, q)-wedge $G(U_W, V_W, E_W)$ is a connected non-induced subgraph that contains a $(p-1, q)$-biclique (or $(p, q-1)$-biclique) and one additional vertex $u \in U_W$ (or $v \in V_W$) which connects at least one vertex in V_W (or U_W). Such a higher-order clustering coefficient measures the probability of a (p, q)-*wedges* becoming a (p, q)-biclique, and it can characterize the internal nature of the bipartite graph data (as confirmed in our experiments). Since the count of (p, q)-wedges can be efficiently computed from the count of (p, q)-bicliques (as shown in Section 6), the key to compute the higher-order clustering coefficient in bipartite graph is to count the (p, q)-bicliques.

Higher-order densest subgraph mining. Finding the densest subgraph from a graph is a fundamental graph ming operator. Recent studies focus mainly on mining higher-order densest subgraph based on k-cliques on traditional graphs [11, 27, 29] and based on (p, q)-bicliques on bipartite graphs [22], because such a higher-order densest subgraph is often a quasi-clique [22, 29] which is very useful for network analysis applications. In bipartite graphs, the (p, q)-biclique densest subgraph is a subgraph with the maximum (p, q)-biclique density, which is defined as the ratio between the count of (p, q)-bicliques in a subgraph S and the number of vertices in S [22]. The exact algorithm to compute the (p, q)-biclique densest subgraph is based on a parametric max-flow procedure, which is often intractable for large bipartite graphs [22]. To obtain a practical solution, we can develop a *peeling* algorithm (as used in [11, 29] for traditional graphs) by iteratively removing the vertex that has the minimum (p, q)-biclique count. Clearly, such a peeling algorithm needs to frequently count the number of (p, q)-bicliques of each vertex. Thus, an efficient approach to count the (p, q)-bicliques is crucial for mining the (p, q)-biclique densest subgraph in bipartite graphs.

Despite of the practical importance of (p, q)-biclique counting, we still lack efficient algorithms to count all bicliques in large bipartite graphs, due to the intrinsic hardness of the biclique counting problem. Indeed, real-world bipartite graphs often contain a huge number of (p, q)-bicliques even for very small p and q. For example, Fig. 1 shows the number of bicliques contained in 7 real-world bipartite graphs given that $p = 4$. As can be seen, the number of bicliques with $p = 4$ can be more than 10^{39} in a medium-sized graph Twitter ($|U| = 175,214$, $|V| = 530,418$, and $|E| = 1,890,661$). As a consequence, it is often intractable to count all (p, q)-bicliques for relatively large p and q in large graphs.

Conference'17, July 2017, Washington, DC, USA

ACM ISBN 978-x-xxxx-xxxx-x/YY/MM…$15.00
https://doi.org/10.1145/nnnnnnn.nnnnnnn

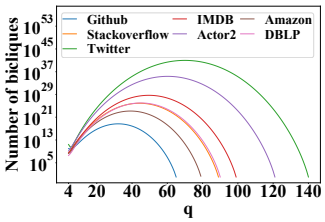

Figure 1: The counts of (p, q)-bicliques for $p = 4$.

The state-of-the-art algorithm to count the (p, q)-biclique is based on a backtracking enumeration technique [33]. The key idea of this algorithm is to maintain a sub-biclique and two candidate vertex sets (the common neighbors of each side of the sub-biclique), and recursively add the vertices from the candidate sets into the sub-biclique to generate a larger biclique. The limitations of this algorithm are twofold: (1) it needs to exhaustively enumerate all (p, q)-bicliques to get the (p, q)-biclique count which is typically very costly for relatively large p and q; and (2) it is mainly tailored for counting (p, q)-bicliques for only a pair of (p, q), and is often intractable to count the bicliques for all possible pairs of (p, q).

To overcome these limitations, we first propose a novel exact algorithm, called EPivoter, to count all bicliques in a bipartite graph G for all pairs of (p, q). A striking feature of EPivoter is that it can count all bicliques for all pairs of (p, q) without of exhaustively enumerating every biclique. To achieve this, we first develop a novel edge-pivoting technique to enumerate maximal bicliques. With such a powerful edge-pivoting technique, we can uniquely represent every biclique by using a set of *large bicliques* (not necessary maximal) which can be enumerated based on our edge-pivoting technique. As a consequence, we can count all bicliques for all pairs of (p, q) in those *large bicliques* using a combinatorial counting method, instead of exhaustively enumerating each biclique. Since enumerating those *large bicliques* is much cheaper than enumerating all bicliques, our algorithm is often tractable to handle large real-world bipartite graphs.

To improve the efficiency, we develop two novel sampling-based algorithms, called ZigZag and ZigZag++, to estimate the counts of all bicliques for all pairs of (p, q). Both ZigZag and ZigZag++ are based on a newly-developed h-zigzag sampling technique, where an h-zigzag is an vertex-ordered simple path in G with length $2h - 1$ and $h = \min\{p, q\}$. It is easy to see that any (p, q)-biclique of G contains at least one h-zigzag, thus we can estimate the number of (p, q)-bicliques by sampling h-zigzags. To obtain uniform h-zigzag samples, we propose a dynamic programming (DP) based h-zigzag counting and sampling algorithm. We show that the time complexity of our DP-based sampling algorithm is bounded by $O(h|E|)$, thus it is very efficient when h is not very large. In addition, to further improve the sampling performance, we also propose a hybrid framework by integrating both our exact algorithm and sampling-based algorithms. The hybrid framework is based on the following observation: the sampling-based algorithms often work well in the dense region of the bipartite graph (because in the dense region, an h-zigzag is likely to be contained in a certain biclique, thus improving the sampling performance), while the exact algorithm performs very well in the sparse region of the graph (because in the sparse region, the number of *large bicliques* is not very large). Therefore, to achieve better performance, the hybrid framework uses the exact algorithm to count bicliques in the sparse region of the graph, while leverages the sampling-based algorithms to process the dense region of the graph. We also devise an efficient and effective algorithm to partition the bipartite graph into a sparse region and a dense region. The results of extensive experiments demonstrate the high efficiency of our solutions. In summary, the main contributions of this paper are as follows.

Novel exact algorithms. We proposed a novel EPivoter algorithm to count all (p, q)-bicliques for all pairs of (p, q). The novelties of EPivoter are twofold: (1) it is the first algorithm that can exactly count all bicliques without exhaustively enumerating each biclique; and (2) it relies on a new edge-pivoting technique which can also be used to enumerate all maximal bicliques. We believe that our edge-pivoting technique may be of independent interest.

Novel approximation algorithms. We develop two novel approximation algorithms ZigZag and ZigZag++ to estimate the counts of all bicliques for all pairs of (p, q). The novelties of our two approximation algorithms lie in that (1) both of them are based on a new and efficient DP-based h-zigzag sampling technique, and (2) both of them are the first algorithm that can provably approximate the number of (p, q)-bicliques for all pairs of (p, q). In addition, to further improve the accuracy of the approximation algorithms, we also present a hybrid framework by integrating our exact algorithm and approximation algorithms based on a carefully-designed graph partition technique.

Extensive experiments. We conduct extensive experiments on 7 real-life bipartite graphs to evaluate our algorithms. The results show that (1) our exact algorithm is very efficient to count all bicliques and it is more than two orders magnitude faster than the state-of-the-art (SOTA) algorithm. For example, on Actor2 ($|U| = 303,617$, $|V| = 896,302$, and $|E| = 3,782,463$), EPivoter takes only 49 seconds to count all bicliques for all pairs of (p, q), while the SOTA algorithm consumes 12,476 seconds. (2) All our approximation algorithms are not only very efficient, but also pretty accurate to estimate the counts of (p, q)-bicliques with $h = \min\{p, q\} \leq 10$. For example, on Actor2, our best approximation algorithm teaks only 15 seconds, while the SOTA algorithm uses 9,015 seconds. Moreover, the average estimator error of our best approximation algorithm can be lower than 0.7% on Actor2. (3) Even when estimating the count of the (p, q)-bicliques for only one pair of (p, q), our exact and approximation algorithms are still much faster than the SOTA algorithm for relatively large p and q (e.g., $p = 8$ and $q = 8$). In addition, we also conduct two application experiments including the fast computation of higher-order clustering coefficient on bipartite graphs and computing the (p, q)-biclique densest subgraph by a newly-developed peeling-based $\frac{1}{p+q}$-approximate algorithm. The experiment results demonstrate the effectiveness of our biclique counting techniques.

2 PRELIMINARIES

Let $G = (U, V, E)$ be a bipartite graph, where U and V are two disjoint set of vertices and $E = \{e(u, v)|u \in U, v \in V\}$ denotes the set of edges. For each vertex u in U (or V), its neighbor set is defined as $N(u, G) = \{v|e(u, v) \in E\}$. For a vertex set S, the set of the common neighbors of S is defined as $N(S, G)$, i.e., $N(S, G) = \cap_{u \in S} N(u, G)$. Let $d(u, G)$ be the degree of u in G, i.e. $d(u, G) = |N(u, G)|$. If the

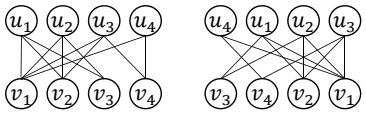

(a) A bipartite graph (b) Degree-ordered graph

Figure 2: A running example

context is clear, $N(u, G)$, $N(S, G)$ and $d(u, G)$ are abbreviated as $N(u)$, $N(S)$ and $d(u)$, respectively. In addition, we also define the set of neighbors of an edge $e(u, v) \in E$ denoted by $N(e(u, v), G)$ as $N(e(u, v), G) \triangleq \{e(u', v') \in E | u' \in N(v) \setminus \{u\}, v' \in N(u) \setminus \{v\}\}$.

Denote by $\{u_1, u_2, ..., u_{n_1}\}$ ($\{v_1, v_2, ..., v_{n_2}\}$) a non-decreasing ordering of vertices in U (V) with respect to (w.r.t.) the vertices' degrees (break ties by vertex IDs), where $n_1 = |U|$ ($n_2 = |V|$). For convenience, we refer to such an ordering as a degree ordering $\prec_d$. With such a degree ordering $\prec_d$, we have $d(u_i) \leq d(u_j)$ ($d(v_i) \leq d(v_j)$) for each u_i and u_j (v_i and v_j) if $u_i \prec_d u_j$ ($v_i \prec_d v_j$). Then, based on $\prec_d$, we define the set of *ordering neighbors* of v w.r.t. a reference vertex u_i as $N^{\succ u_i}(v, G) \triangleq \{u_j | e(u_j, v) \in E, u_i \prec_d u_j\}$, which includes the neighbors of v in G with ranks higher than u_i's rank according to the degree ordering. Similarly, $N^{\succ v_i}(u, G) \triangleq \{v_j | e(u, v_j) \in E, v_i \prec_d v_j\}$ is defined as the neighbors of u in G w.r.t. v_i. Based on these definitions, we further define the set of ordering neighbors of an edge $e(u_i, v_j)$ as $\vec{N}(e(u_i, v_j)) \triangleq \{e(u_{i'}, v_{j'}) \in E | u_{i'} \in N^{\succ u_i}(v_j), v_{j'} \in N^{\succ v_j}(u_i)\}$.

Example 2.1. Consider a bipartite graph shown in Fig. 2(a). The set of neighbors of u_1 is $N(u_1, G) = \{v_1, v_2, v_3\}$, and the set of neighbors of v_2 is $N(v_2, G) = \{u_1, u_2, u_3\}$. The set of common neighbors of a vertex set $\{u_1, u_4\}$ is $N(\{u_1, u_4\}) = N(u_1, G) \cap N(u_4, G) = \{v_1\}$. By definition, it is easy to derive that the set of neighbors of an edge $e(u_1, v_2)$ is $N(e(u_1, v_2)) = \{e(u_2, v_1), e(u_2, v_3), e(u_3, v_1)\}$. Clearly, both (u_4, u_1, u_2, u_3) and (v_3, v_4, v_2, v_1) are valid degree orderings by our definition. It is easy to see that Fig. 2(b) is a *degree-ordered* bipartite graph of Fig 2(a). Based on the degree ordering, we have $N^{\succ v_2}(u_1) = \{v_1\}$ and $N^{\succ u_1}(v_2) = \{u_2, u_3\}$. Further, we can derive that the set of ordering neighbors of an edge (u_1, v_2) is $\vec{N}(e(u_1, v_2)) = \{e(u_2, v_1), e(u_3, v_1)\}$.

Definition 2.2. Given a bipartite graph $G(U, V, E)$, a biclique in G is a complete subgraph with a pair of vertex sets (X, Y) where $X \subseteq U, Y \subseteq V$ and $\forall u \in X, \forall v \in Y, e(u, v) \in E$.

A biclique is maximal if no vertex can be added into it to generate a larger biclique. A (p, q)-biclique (X, Y) is a biclique with $|X| = p$ and $|Y| = q$. In this paper, we investigate two problems on (p, q)-biclique counting: (1) the first problem is to compute the number of (p, q)-bicliques in a bipartite graph G with a given p and q; and (2) the second problem is to simultaneously count the (p, q)-bicliques in G for every pair of p and q.

As discussed in Section 1, the first problem is very hard for large p and q (e.g., $p \geq 10$, $q \geq 10$) due to the exponential blowup of the biclique counts. For example, in the Twitter dataset ($|U| = 175,214$, $|V| = 530,418$, $|E| = 1,890,661$), even for small p and q, the number of (p, q)-bicliques can be extremely large (for $p = 2$ and $q = 2$, the $(2, 2)$-biclique count is more than 2×10^8; and for $p = 5$ and $q = 5$, the $(5, 5)$-biclique count is around 1×10^{13}). Clearly, the second problem is much more difficult than the first problem, as it requires to count all (p, q)-bicliques for every pair of p and q.

Existing solution and its limitation. The state-of-the-art algorithm [33] to solve our problems is based on exhaustively enumerating all (p, q)-bicliques, which is often intractable for relatively-large p and q in large bipartite graphs. This is because the number of (p, q)-bicliques can be an astronomical number for relatively-large (p, q)-bicliques, and thus any enumeration-based technique that needs to list all (p, q)-bicliques is doomed to failure. Moreover, the algorithm proposed in [33] is mainly devised to count the (p, q)-bicliques for a given p and q. When using such an algorithm to solve our second problem, it needs to invoke the algorithm multiple times for all possible p and q, which is clearly very costly.

To overcome the challenges in our problems, the key is to avoid exhaustively enumeration of all (p, q)-bicliques. In the following sections, we will propose an exact counting algorithm and a sampling-based approximation algorithm to achieve this goal.

3 THE PROPOSED EPIVOTER ALGORITHM

In this section, we propose a novel exact algorithm, called EPivoter, to count the (p, q)-bicliques for all p and q. The EPivoter algorithm is inspired by the PIVOTER algorithm which was originally designed to count the k-cliques in traditional graphs [14]. Specifically, PIVOTER uses the classic pivoting technique in maximal clique enumeration [6, 28] to generate a so-called *succinct clique tree* (SCT) structure which can uniquely encode every k-clique in a compact way. Based on this *SCT* structure, PIVOTER then counts all k-cliques using a combinatorial counting method, instead of exhaustively enumerating all k-cliques. However, extending the idea of PIVOTER for counting bicliques is a quite non-trivial task, because there is no similar pivoting technique in existing maximal clique enumeration algorithms [1, 23, 38] that can be used to construct a *SCT-style* structure. Moreover, even if we have a pivoting technique, the construction of a unique representation for every (p, q)-biclique is still very challenging, because a biclique has two sides of vertices and both of them are needed to be uniquely encoded. Indeed, as we shown in Section 3.2, we need to consider 6 different and more complicated cases to encode every (p, q)-biclique, while it is sufficient to consider two simple cases to encode each k-clique in PIVOTER [14] (i.e, a k-clique either contains the pivot vertex or not).

To overcome these problems, we first develop a new maximal biclique enumeration algorithm with a carefully-designed edge-pivoting technique, which selects an edge for pivoting instead of a vertex in each recursion. Based on this edge-pivoting technique, we then propose a representation method which can uniquely encode every (p, q)-clique. Armed with such a representation approach, we are able to count the (p, q)-bilciques for all p and q using a combinatorial counting method. Below, we detail our solutions.

3.1 New maximal biclique enumeration algorithm

In this subsection, we propose a new backtracking algorithm called EPMBCE to enumerate all maximal bicliques. The novelty of EPMBCE lies in the facts that (1) in each recursion, EPMBCE selects an edge to expand the biclique, while all existing algorithms choose a vertex to expand the biclique [1, 23, 38]; and (2) EPMBCE is integrated

Algorithm 1: EPMBCE

```
Input: A bipartite graph G = (U, V, E)
Output: All maximal bicliques in G
1  C ← ∅;
2  MBCE (U, V, ∅, ∅);
3  return C  Procedure MBCE(C_l, C_r, P_l, P_r)
4      Denote by G'(C_l, C_r, E') the subgraph of G, where
         E' = {e(u, v) ∈ E | u ∈ C_l, v ∈ C_r} ;
5      if E' = ∅ then
6          if C_l ≠ ∅ and C_r ≠ ∅ then
7              Check(P_l ∪ C_l, P_r); Check(P_l, P_r ∪ C_r) ;
8          else Check(P_l ∪ C_l, P_r ∪ C_r) ;
9          return;
10     e(u, v) ← max_{e(u,v)∈E'} |N(e(u, v), G')| ;
11     if C_l \ N(v) ≠ ∅ then Check(P_l ∪ C_l, P_r) ;
12     if C_r \ N(u) ≠ ∅ then Check(P_l, P_r ∪ C_r) ;
13     Reset the IDs of vertices in C_l and C_r such that for each u' ∈ C_l \ N(v),
         v' ∈ C_r \ N(u), we have u' ≺ u'' and v' ≺ v'' if u'' ∈ C_l ∩ N(v) and
         v'' ∈ C_r ∩ N(u) ;
14     foreach e(u', v') ∈ E' s.t. (u' ∉ N(v) or v' ∉ N(u)) do
15         C'_l ← C_l ∩ N^{≻u'}(v'); C'_r ← C_r ∩ N^{≻v'}(u') ;
16         MBCE(C'_l, C'_r, P_l ∪ {u'}, P_l ∪ {v'}) ;
17     C'_l ← C_l ∩ N(v) \ {u}; C'_r ← C_r ∩ N(u) \ {v} ;
18     MBCE(C'_l, C'_r, P_l ∪ {u}, P_l ∪ {v}) ;
19 Procedure Check(X, Y)
20     if (X, Y) is maximal then
21         C ← C ∪ {(X, Y)}
```

with a newly-developed edge-pivoting technique to further reduce the search space.

Specifically, the basic idea of our algorithm is that for every maximal biclique (L, R) of G, it (1) either contains an edge $e(u, v) \in E$, or (2) does not contain the edge $e(u, v)$. This indicates that we can recursively divide the original problem into two sub-problems: the first one is to enumerate all maximal bicliques containing $e(u, v)$, and the other one is to enumerate all maximal bicliques excluding $e(u, v)$.

However, such a basic algorithm may generate many non-maximal bicliques, which leads to redundant calculations. This is because for any non-maximal biclique, it also satisfies the property that it either contains an edge $e(u, v)$ or does not contain $e(u, v)$. To reduce non-maximal bicliques explored by the enumeration procedure, we further present a novel edge-pivoting technique, which is shown in the following theorem.

THEOREM 3.1. *Given a bipartite graph $G(U, V, E)$ with $|E| > 0$. If we choose an edge $e(u, v) \in E$ as the pivot edge, every maximal biclique must contain at least one edge in $\{e(u, v)\} \cup \{e(u', v') \in E | u' \notin N(v)$ or $v' \notin N(u)\}$.*

PROOF. For the maximal bicliques containing the pivot edge $e(u, v)$, the proof clearly holds. For the maximal bicliques that do not contain $e(u, v)$, it is easy to derive that they must contain at least one vertex in $\{e(u', v') \in E | u' \notin N(v)$ or $v' \notin N(u)\}$, otherwise adding $e(u, v)$ to them will generate larger bicliques. □

Equipped with Theorem 3.1, we can easily derive that for any maximal biclique in G, it either contains an edge $e(u, v)$, or contains an edge $e(u', v')$ with $u' \notin N(v)$ or $v' \notin N(u)$. Based on this, we can develop an edge-pivoting technique to further improve our basic *edge-based* enumeration algorithm. Specifically, we first select an edge $e(u, v)$ in E as a pivot, and then find all maximal bicliques in G by only enumerating the maximal bicliques containing each edge in $\{e(u, v)\} \cup \{e(u', v') \in E | u' \notin N(v)$ or $v' \notin N(u)\}$. The detailed pseudo-code is shown in Algorithm 1.

In Algorithm 1, it invokes the MBCE procedure to recursively enumerate all maximal bicliques (line 2). Specifically, MBCE admits four parameters C_l, C_r, P_l, and P_l, where $(P_l \subset U, P_r \subset V)$ is the partial biclique, and (C_l, C_r) is the candidate set such that every vertex $u \in C_l$ $(v \in C_r)$ can be added to P_l (P_r) to form a larger biclique. Let E' be the set of edges in the subgraph G' of G induced by the candidate sets (C_l, C_r) (line 4). If E' is empty (line 5), the algorithm first determines whether the candidate sets are empty, and then adds the non-empty candidate sets into the current biclique to generate a larger biclique and also checks the maximality of the generated bicliques (lines 6-8). After that, the algorithm can terminate the current recursion, as in this case no pivot can be used to further branching (line 9). If E' is non-empty, the algorithm chooses the edge $e(u, v)$ which has the maximum number of neighbors in the candidate set as the pivot edge (line 10), because such a pivot edge can prune the most number of candidates. Then, according to Theorem 3.1, each edge in $\{e(u, v)\} \cup \{e(u', v') \in E' | u' \notin N(v)$ or $v' \notin N(u)\}$ can be used to expand the current partial biclique (P_l, P_r), and the corresponding sub-recursive calls are further invoked to continue the enumeration (lines 13-16 correspond to the non-neighbors and lines 17-18 correspond to the pivot edge). The notation $N^{\succ u'}(v')$ and $N^{\succ v'}(u')$ in line 15 is the set of ordering neighbors $\{u_j | e(u_j, v') \in E, u' \prec u_j\}$ and $\{v_j | e(u', v_j) \in E, v' \prec v_j\}$ defined in Section 2. Note that in line 20, the algorithm can check the maximality using existing techniques in maximal biclique enumeration algorithms [1, 23, 38]. The correctness of Algorithm 1 is shown in the following theorem.

THEOREM 3.2. *Algorithm 1 correctly outputs all maximal bicliques of a given bipartite graph G.*

PROOF. In the recursive tree of Algorithm 1, we label the tree node, which corresponds to the recursive call including the pivot edge $e(u, v)$ (line 19), as the *p-node*, and the other non-*p-node* in the recursive tree as the *h-node*. Without loss of generality, we first prove that a randomly chosen maximal biclique (X, Y) that $|X| > 0, |Y| > 0$ must be enumerated by the algorithm. Denote by $e_p = e(u, v)$ the pivot edge. According to Theorem 3.1, (X, Y) must (1) contain e_p, or (2) contain at least an edge in $\{e(u', v') \in E | u' \notin N(v)$ or $v' \notin N(u)\}$ if $|X| > 0, |Y| > 0$.

For the case (1), if (X, Y) contains e_p, other vertices in (X, Y) must be the neighbors of e_p. This means that $X' = X \setminus \{u\} \subseteq C'_l, Y' = Y \setminus \{v\} \subseteq C'_r$, where C'_l and C'_r are the results obtained by line 17 of Algorithm 1. Thus, if the *p-node* can enumerate (X', Y') in the subgraph G' of G induced by (C'_l, C'_r), (X, Y) will be enumerated. Since (X', Y') is also maximal in G', the result in Theorem 3.1 can also be applied. The recursion continues until reaching a certain child node with $(X^* \subset X, Y^* \subset Y)$ where $X^* = \emptyset$ or $Y^* = \emptyset$. In this recursion, we let (C_l, C_r) be the candidate set, where $X^* \subseteq C_l, Y^* \subseteq C_r$. Note that we must have $C_l = X^*$ $(C_r = Y^*)$ if $Y^* = \emptyset$ $(X^* = \emptyset)$, since in each recursive call of Algorithm 1, both $(P_l \cup C_l) \subseteq N(P_r)$ and $(P_r \cup C_r) \subseteq N(P_l)$ are always satisfied. When $Y^* = \emptyset$ $(X^* = \emptyset)$, we have $X = N(Y) = N(P_r) \supseteq (P_l \cup C_l)$ $(Y \supseteq (P_r \cup C_r))$. Finally, the result (X, Y) can be obtained by lines 6-8 and lines 11-12 of Algorithm 1. Thus, we prove the case that e_p is contained in (X, Y).

Second, we prove the theorem for the case of (X, Y) containing some edges in $\{e(u', v') \in E | u' \notin N(v) \text{ or } v' \notin N(u)\}$. When the first edge $e(u', v')$ of (X, Y) is chosen, other edges in $(X \setminus \{u'\}, Y \setminus \{v'\})$ must be contained in the subgraph of G induced by (C_l', C_r'), where C_l' and C_r' are the results obtained by line 15 of Algorithm 1. This is because for each edge $e(u'', v'')$ in $(X \setminus \{u'\}, Y \setminus \{v'\})$, we always have $u'' > u'$ and $v'' > v'$ by line 14. Similarly, the original problem can be converted to a problem of finding $(X \setminus \{u'\}, Y \setminus \{v'\})$ in the *h-node*, and the recursion continues until it reach a child node with $(X^* \subset X, Y^* \subset Y)$, where $X^* = \emptyset$ or $Y^* = \emptyset$. Thus, similar arguments as the case (1) can also be used to prove the case (2).

By the Check procedure, all non-maximal bicliques are omitted. And it is easy to see that each potential maximal biclique cannot be checked twice by the Check procedure. Putting all it together, the theorem is established. □

The time and space complexity of Algorithm 1 are shown in the following theorem.

THEOREM 3.3. *Given a bipartite graph $G(U, V, E)$, the worst-case time and space complexity of Algorithm 1 is $O(3^{|E|/3})$ and $O(|E| + |U| + |V| + d_{\max}^2)$ respectively, where $d_{\max}$ is the maximal degree among all vertices.*

PROOF. Let $e_p(u, v)$ be the pivot edge. Denote by E' the set of non-neighbor edges of e_p, i.e. $E' = \{e(u', v') | u' \in U \setminus N(v) \text{ or } v' \in V \setminus N(u)\}$. Let $e_1 = |N(e_p)|$, $e_2 = |N(u)| + |N(v)|$ and $e_3 = |E'|$. Here e_1 is the size of neighbors of e_p, e_2 is the numbers of edges connecting u and v, and e_3 is the size of non-neighbors of e_p. Clearly, we have $e_1 + e_2 + e_3 = |E|$. Let $T(|E|)$ be the time complexity of MBCE with the input E. We have

$$T(|E|) = T(|N(e_p)|) + \sum_{e \in E'} T(|N(e)|) + p_1|E|^2, \tag{1}$$

where $T(|N(e_p)|)$ is the time cost spent on the p-node, $\sum_{e \in E'} T(|N(e)|)$ is total time costs spent on the h-nodes, and $p_1|E|^2$ is the time taken to select the e_p with $p_1 > 0$. Since the pivot edge e_p is the edge with maximum $|N(e)|$, we have $|N(e)| < |N(e_p)| = e_1, \forall e \in E'$. Further, we can derive that

$$\begin{aligned} T(|E|) &\leq (e_3 + 1)T(e_1) + p_1|E|^2 \\ &= (e_3 + 1)T(|E| - e_2 - e_3) + p_1|E|^2 \\ &\leq (e_3 + 1)T(|E| - (e_3 + 1)) + p_1|E|^2 \end{aligned} \tag{2}$$

Clearly, $|E| - (e_3 + 1) \leq |E| - 1$. By applying the results established in [28], we can derive that the time complexity of our algorithm is $O(3^{|E|/3})$.

For each search node with parameter (C_l, C_r), it takes $|C_l| + |C_r|$ space. Apart from the search node at the level-0 with $|C_l| = |U|, |C_r| = |V|$, we have $|C_l| < d_{\max}$ and $|C_r| < d_{\max}$ for other child nodes. Furthermore, both C_l and C_r decrease at least one 1 for each child node, as the selected edge is removed. Thus, the search depth is bounded by $O(d_{\max})$. The space usage for storing (C_l, C_r) in each search branch is $O(d_{\max}^2)$, and the graph takes $O(|E| + |U| + |V|)$ space. Putting all it together, the space complexity of Algorithm 1 is $O(|E| + |U| + |V| + d_{\max}^2)$. □

Algorithm 2: BCEUnique

Input: A bipartite graph $G(U, V, E)$
Output: The unique representation for each biclique

1 **Procedure** BCEUnique$(C_l, C_r, \tilde{P}_l, H_l, \tilde{P}_r, H_r)$
2 Denote by $G'(C_l, C_r, E')$ the subgraph of G, where $E' = \{e(u, v) \in E | u \in C_l, v \in C_r\}$;
3 **if** $E' = \emptyset$ **then**
4 **if** $C_l \neq \emptyset$ *and* $C_r \neq \emptyset$ **then**
5 Represent$(\tilde{P}_l \cup C_l, H_l, \tilde{P}_r, H_r)$;
6 **for** *each non-empty subset set S of* C_r **do**
7 Represent$(\tilde{P}_l, H_l, \tilde{P}_r, H_r \cup S)$;
8 **else** Represent$(\tilde{P}_l \cup C_l, H_l, \tilde{P}_r \cup C_r, H_r)$;
9 **return**;
10 $e(u, v) \leftarrow \max_{e(u,v) \in E'} |N(e(u, v), G')|$;
11 Reset the IDs of vertices in C_l and C_r such that for each $u' \in C_l \setminus N(v)$, $v' \in C_r \setminus N(u)$, we have $u' < u''$ and $v' < v''$ if $u'' \in C_l \cap N(v)$ and $v'' \in C_r \cap N(u)$;
12 **foreach** $e(u', v') \in E'$ *s.t.* $(u' \notin N(v)$ *or* $v' \notin N(u))$ **do**
13 $C_l' \leftarrow C_l \cap N^{>u'}(v'); C_r' \leftarrow C_r \cap N^{>v'}(u')$;
14 BCEUnique$(C_l', C_r', \tilde{P}_l, H_l \cup \{u'\}, \tilde{P}_r, H_r \cup \{v'\})$;
15 $C_l' \leftarrow C_l \cap N(v) \setminus \{u\}; C_r' \leftarrow C_r \cap N(u) \setminus \{v\}$;
16 BCEUnique$(C_l', C_r', \tilde{P}_l \cup \{u\}, H_l, \tilde{P}_r \cup \{v\}, H_r)$;
17 **foreach** $w \in C_l \setminus N(v)$ **do**
18 $C_l \leftarrow C_l \setminus \{w\}$;
19 Represent$(\tilde{P}_l \cup C_l, H_l \cup \{w\}, \tilde{P}_r, H_r)$;
20 **foreach** $w \in C_r \setminus N(u)$ **do**
21 $C_r \leftarrow C_r \setminus \{w\}$;
22 Represent$(\tilde{P}_l, H_l, \tilde{P}_r \cup C_r, H_r \cup \{w\})$;
23 **Procedure** Represent$(\tilde{P}_l, H_l, \tilde{P}_r, H_r)$
24 **foreach** *subset X of* $\tilde{P}_l$ **do**
25 **foreach** *subset Y of* $\tilde{P}_r$ **do**
26 $(X \cup H_l, Y \cup H_r)$ is an unique biclique;

After obtaining all maximal bicliques, we may count the (p, q)-cliques for all p and q in the set of all maximal bicliques using a combinatorial counting technique, as every bipartite subgraph of a maximal biclique is a (p, q)-clique for a particular p and q. However, such a method may count a (p, q)-clique multiple times, because a (p, q)-clique can be located in many maximal bicliques. A natural question is that can we have an algorithm that can avoid repeatedly count the (p, q)-cliques based on the maximal bicliques? In the following sections, we answer this question affirmatively by using our edge-pivoting technique.

3.2 Unique representation for each biclique

In this subsection, we establish a unique representation for each biclique based on our edge-pivoting technique. Below, we first classify all bicliques into six categories based on the pivot edge, and then we will show how to uniquely represent all these types of bicliques based on our maximal clique enumeration technique.

THEOREM 3.4. *Let $e_p = e(u, v)$ be the pivot edge, and $N(e_p, G)$ be the set of neighbor edges of e_p in G. Then, each biclique ((including $(p, 0)$-biclique and $(0, q)$-biclique) must belong to one of the following six categories.*

(1) *It contains u and v, and the other vertices are included in the subgraph induced by $N(e_p, G)$.*
(2) *It contains u but v, and the other vertices are included in the subgraph induced by $N(e_p, G)$.*
(3) *It contains v but u, and the other vertices are included in the subgraph induced by $N(e_p, G)$.*

(4) *It does not contain u or v, with all vertices included in the subgraph induced by* $N(e_p, G)$.
(5) *It only contains vertices in* U *(or* V*), and contains at least one vertex in* $U \setminus N(v)$ *(or* $V \setminus N(u)$*).*
(6) *It contains at least one vertex in* $U \setminus N(v)$ *or* $V \setminus N(u)$*, and includes at least one edge in* $\{e(u', v') \in E | u' \in U \setminus N(v)$ *or* $v' \in V \setminus N(u)\}$.

PROOF. By definition, $U \cup V \setminus N(u) \setminus N(v)$ is a set of non-neighbor vertices of u or v. Then, we can initially partition all bicliques into two types by determining whether they contain vertices in $U \cup V \setminus N(u) \setminus N(v)$, i.e. contain non-neighbor vertices of the pivot. If so, we can further divide the bicliques into four cases, corresponding to the cases (1)-(4), by considering whether they contain u and v. If not, we can also further partition the bicliques into two cases, corresponding to the cases (5)-(6), by considering whether they contain edges. □

Let G' be the subgraph of $G(C_l, C_r)$ induced by $N(e_p, G(C_l, C_r))$ ($G(C_l, C_r)$ is a bipartite subgraph of G induced by the candidate sets (C_l, C_r)). Then, by Theorem 3.4, any biclique of G is either contained in $G' \cup \{e_p\}$ (cases (1)-(4)) or includes a vertex outside of $G' \cup \{e_p\}$ (cases (5)-(6)). It is easy to see that all the bicliques belonging to cases (1)-(4) must be contained in the maximal bicliques enumerated in the enumeration branch of Algorithm 1 that includes e_p (line 19 of Algorithm 1). Similarly, we can easily derive that each biclique belonging to case (6) must be contained in a maximal biclique enumerated in the enumeration branch of Algorithm 1 that includes a non-neighbor edge of e_p (lines 15-17 of Algorithm 1). Note that the bicliques belonging to case (5) cannot be directly enumerated by Algorithm 1. However, by definition, we can see that case (5) only contains the bicliques that have one-side vertices and the other side is an empty set. In other words, only the $(p, 0)$-bicliques or $(0, q)$-bicliques belong to the case (5). Interestingly, such bicliques can be computed by using a combinatorial counting method, because in Algorithm 1, these bicliques must be included in C_r (or C_r) and contain at least one vertex in $C_l \setminus N(v)$ (or $C_l \setminus N(u)$), where $e(u, v)$ is the pivot edge.

Based on the above analysis, an unique representation for each biclique of G can be obtained based on the enumeration tree generated by our edge-pivoting technique. Specifically, for the current partial biclique (P_l, P_r) in each recursion of Algorithm 1, we divide the vertex set P_l into two subset $\tilde{P}_l$ and H_l, where $\tilde{P}_l$ only contains the vertices of all the selected pivot edges (in the current recursion, there may exist several pivot edges that have already added into (P_l, P_r) in the previous recursions) and H_l contains the remaining vertices in P_l (i.e., $P_l = \tilde{P}_l \cup H_l$). Similarly, we partition P_r as $\tilde{P}_r$ and H_r. With these notations, we can easily distinguish the bicliques. This is because whenever a vertex in $\tilde{P}_l$ or $\tilde{P}_r$ is selected or not, it can yield a different biclique (cases (1)-(4) of Theorem 3.4). In other words, any combination of the vertices in $\tilde{P}_l$ and $\tilde{P}_r$ can generate a different biclique. Algorithm 2 gives a detailed implementation to uniquely represent the bicliques in G based on our edge-pivoting technique.

The general procedure of Algorithm 2 is very similar to Algorithm 1, as both of them are based on our edge-pivoting technique. The main differences are summarized as follows. First, to maintain the current partial biclique in each recursion, Algorithm 2 requires four sets $\tilde{P}_l$, $\tilde{P}_r$, H_l and H_r as we defined before. The algorithm will add the vertices of pivot edges (non-pivot edges) into $\tilde{P}_l$ and $\tilde{P}_r$ (H_l and H_r) for the next recursion (see line 16 and line 14). Second, unlike Algorithm 1, there is no need to check the maximality of the biclique in Algorithm 2. Instead, when there is no edges in the candidate set (C_l, C_r), Algorithm 2 terminates the recursion and invokes the Represent procedure to uniquely represent each biclique contained in the current *enumerated biclique* by using a combinatorial technique (see lines 3-9 and lines 23-26). For convenience, in Algorithm 2, we refer to the input biclique of the Represent procedure, denoted by $(\tilde{P}_l \cup H_l \cup C_l, \tilde{P}_r \cup H_r)$, as the *enumerated biclique*. The set of all these *enumerated bicliques* uniquely encode every biclique in G. Note that in line 4 of Algorithm 2, when $C_l \neq \emptyset$ and $C_r \neq \emptyset$, there are two kinds of bicliques, one included in $(\tilde{P}_l \cup H_l \cup C_l, \tilde{P}_r \cup H_r)$ and the other contained in $(\tilde{P}_l \cup H_l, \tilde{P}_r \cup H_r \cup C_r)$. Both of them can represent the bicliques that are contained in $(\tilde{P}_l \cup H_l, \tilde{P}_r \cup H_r)$. Therefore, after obtaining all bicliques included in $(\tilde{P}_l \cup H_l \cup C_l, \tilde{P}_r \cup H_r)$, the other bicliques must contain at least one vertex in C_r to avoid duplicate representation (lines 6-7). In addition, for the bicliques containing at least one vertex only in $C_l \setminus N(v)$ (or only in $C_r \setminus N(u)$), which corresponds to the bicliques belonging to the case (5) in Theorem 3.4, we also need to invoke Represent to uniquely represent them (lines 17-22 of Algorithm 2). The following theorem shows that every biclique in G can be uniquely represented by Algorithm 2.

THEOREM 3.5. *Algorithm 2 uniquely represents every biclique in the bipartite graph G.*

PROOF. Without lose of generality, we randomly choose a (p, q)-biclique (L, R) with $|L| = p$ and $|R| = q$ and show that there is only one $(X \cup H_l, Y \cup H_r)$ for each *enumerated biclique* $(\tilde{P}_l \cup H_l, \tilde{P}_r \cup H_r)$ such that $L = X \cup H_l$ and $R = Y \cup H_r$. Denote by $(\tilde{P}_l^i, H_l^i, C_l^i, \tilde{P}_r^i, H_r^i, C_r^i)$ the parameters of a recursion node in the enumeration tree of Algorithm 2 at level i. Below, we prove the theorem from two aspects: *Existence* and *Uniqueness*.

Existence. We call the level i of the enumeration tree holding a state $\mathbb{S}_i$ if $L = X^i \cup H_l^i, R = Y^i \cup H_r^i$ where $X^i \subseteq \tilde{P}_l^i \cup C_l^i$ and $Y^i \subseteq \tilde{P}_r^i \cup C_r^i$. When $i = 0$, we have $\tilde{P}_l^0 = H_l^0 = \tilde{P}_r^0 = H_r^0 = \emptyset$ and $C_l^0 = U, C_r^0 = V$, so the base case $\mathbb{S}_0$ holds. We claim that the property of holding a state $\mathbb{S}_i$ satisfies transitivity. That is, if the level-i node in the enumeration tree holds state $\mathbb{S}_i$, then there must exists a child node of level-$(i+1)$ holds $\mathbb{S}_{i+1}$, i.e., $L = X^{i+1} \cup H_l^{i+1}, R = Y^{i+1} \cup H_r^{i+1}$ where $X^{i+1} \subseteq \tilde{P}_l^{i+1} \cup C_l^{i+1}$ and $Y^{i+1} \subseteq \tilde{P}_r^{i+1} \cup C_r^{i+1}$. With such a transitivity property, we can easily prove that $\mathbb{S}$ still holds when C_l and C_r goes to empty, i.e. $L = X \cup H_l, R = Y \cup H_r$ where $X \subseteq \tilde{P}_l$ and $Y \subseteq \tilde{P}_r$. Below, we prove that the property of holding a state $\mathbb{S}_i$ satisfies transitivity.

According to Theorem 3.4, there exists six cases. For cases (1)-(4) ((L, R) does not contain non-neighbors of the pivot edge), the pivot edge from (C_l^i, C_r^i) is added into the current partial biclique $(\tilde{P}_l^i, \tilde{P}_r^i)$, and (H_l^i, H_r^i) does not change. Clearly, in these cases, the state $\mathbb{S}_{i+1}$ holds. For case (6) ((L, R) contains non-neighbors of the pivot edge), the first non-neighbor edge $e(u, v) \in (C_l^i, C_r^i)$ is pushed into (H_l^i, H_r^i), with $C_l^{i+1} = C_l^i \cap N^{>u}(v), C_r^{i+1} = C_r^i \cap N^{>v}(u)$. Note that $e(u, v)$ is the first non-neighbor edge of the pivot edge contained in (L, R), so it has $L \setminus X^i \setminus H_l^{i+1} \subseteq C_l^i \cap N^{>u}(v), R \setminus Y^i \setminus H_r^{i+1} \subseteq C_r^i \cap N^{>v}(u)$. Thus $\mathbb{S}_{i+1}$ holds for case (6). For case (5), we have $L \subseteq X^i \cup H_l^i$

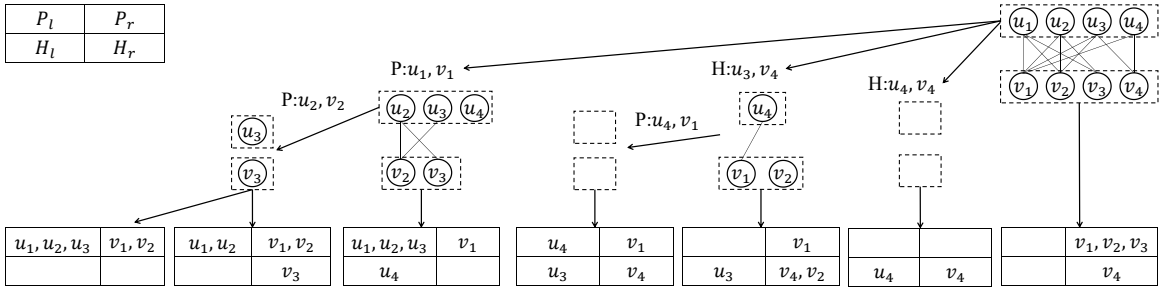

Figure 3: Illustration of the unique representation of each biclique

where $X^i \subseteq \tilde{P}_l^i$ and $R = Y^i \cup H_r^i$ where $Y^i \subseteq P_r^i \cup C_r^i$ (or $L = X^i \cup H_l^i$ where $X^i \subseteq \tilde{P}_l^i \cup C_l^i$ and $R = Y^i \cup H_r^i$ where $Y^i \subseteq \tilde{P}_r^i$). Y^i (or X^i) contains non-neighbor vertices of the pivot edge. Lines 3-8 or 17-22 of Algorithm 2 enumerate the power set of C_r (or C_l) and ensure the existence of non-neighbor vertices in these power set.

Uniqueness. We then prove that (L, R) can be represented uniquely. For each pair of branches of Algorithm 2, there must exist a lowest common search (LCS) node between them in the enumeration tree. If one branch contains the pivot edge $e(u, v)$ in the LCS node, the other branch must exclude $e(u, v)$ and also must contain other edges in H_l and H_r, resulting in no duplicate representation. If both of the branches do not contain the pivot edge, the edge added into (H_l, H_r) is removed after the first branch, resulting in a unique representation in the second branch. For the branches stopping at lines 17-22 of Algorithm 2, which corresponds to case (5) of Theorem 3.4, they must contain non-neighbor vertices of the pivot only in $C_l \setminus N(v)$ or only in $C_r \setminus N(u)$. Thus these branches must have unique representation. As a result, each (L, R) is represented uniquely. □

The following example illustrates how Algorithm 2 works.

Example 3.6. Fig. 3 shows an example of the unique representation for every biclique. The seven quadrille tables at the bottom of Fig. 3 are the 7 *enumerated bicliques* obtained by Algorithm 2, which are input into the Represent procedure to represent all bicliques. Here we illustrate how to get the first two *enumerated bicliques* using Algorithm 2. Initially, $\tilde{P}_l, \tilde{P}_r, H_l, H_r$ are set to empty, and C_l and C_r are set as $C_l = \{u_1, u_2, u_3, u_4\}$ and $C_r = \{v_1, v_2, v_3, v_4\}$. First, suppose that $e(u_1, v_1)$ is selected as the pivot edge. The vertices u_1 and v_1 are added into $\tilde{P}_l$ and $\tilde{P}_r$ respectively, and the candidate set is updated to $(C_l, C_r) = (\{u_2, u_3, u_4\}, \{v_2, v_3\})$. Then, the algorithm continues the recursive calls, and another pivot edge (u_2, v_2), selected in the subgraph of G induced by (C_l, C_r), is further added into $\tilde{P}_l$ and $\tilde{P}_r$. After that, we obtain a new candidate set $(C_l, C_r) = (\{u_3\}, \{v_3\})$. In the next recursion with $(P_l, P_r) = (\{u_1, u_2\}, \{v_1, v_2\})$,there does not exist an edge in the subgraph induced by (C_l, C_r). Thus, Algorithm 2 terminates, and generates the *enumerated bicliques*. Since $C_l \neq \emptyset$ and $C_r \neq \emptyset$, the first *enumerated biclique* with $(\tilde{P}_l, \tilde{P}_r) = (\{u_1, u_2, u_3\}, \{v_1.v_2\})$ and $(H_l, H_r) = (\emptyset, \emptyset)$ is directly obtained by pushing all vertices in C_l into $\tilde{P}_l$ (line 5). Then, at least one vertex in C_r is required to add into H_r (lines 6-7). Thus, the second *enumerated biclique* $(\tilde{P}_l, \tilde{P}_r) = (\{u_1, u_2\}, \{v_1.v_2\})$, $(H_l, H_r) = (\emptyset, \{v_3\})$ is obtained. One can further check that all the bicliques in the graph can be uniquely represented by the 7 *enumerated bicliques*.

Algorithm 3: EPivoter

Input: A bipartite graph $G = (U, V, E)$.
Output: The count of (p, q)-bicliques ($C_{p,q}$) for every p and q in G.

1 Sort all vertices in U and V in a non-decreasing order of degree;
2 **for** $e(u, v) \in E$ **do**
3 BCCounting$(N^{>u}(v), N^{>v}(u), \emptyset, \emptyset, \{u\}, \{v\})$;
4 **Procedure** BCCounting$(C_l, C_r, P_l, P_r, H_l, H_r)$
5 **if** $E' = \emptyset$ **then**
6 **if** $C_l \neq \emptyset$ *and* $C_r \neq \emptyset$ **then**
7 Count$(P_l \cup C_l, H_l, P_r, H_r)$;
8 **for** $i = 1$ *to* $|C_r|$ **do**
9 /*choose i vertices of C_r to add into H_r*/
10 **for** $p \geq |H_l|, q \geq |H_r| + i$ **do**
11 $C_{p,q} \leftarrow C_{p,q} + \binom{|P_l|}{p-|H_l|}\binom{|P_r|}{q-|H_r|-i}\binom{|C_r|}{i}$;
12 **else** Count$(P_l \cup C_l, H_l, P_r \cup C_r, H_r)$;
13 **return**;
14 Lines 10-22 of Algorithm 2 (replace the Represent procedure in Algorithm 2 by the Count procedure);
15 **Procedure** Count(P_l, H_l, P_r, H_r)
16 **foreach** $p \geq |H_l|, q \geq |H_r|$ **do**
17 $C_{p,q} \leftarrow C_{p,q} + \binom{|P_l|}{p-|H_l|}\binom{|P_r|}{q-|H_r|}$;

3.3 The EPivoter algorithm

Recall that by Theorem 3.5, each biclique of G must be contained in a uniquely *enumerated biclique* by Algorithm 2, where an *enumerated biclique* denoted by $(\tilde{P}_l \cup H_l, \tilde{P}_r \cup H_r)$ is an input biclique of the Represent procedure of Algorithm 2 (line 23). In this subsection, we propose an algorithm called EPivoter to count the (p, q)-cliques for all p and q using a combinatorial counting method based on Algorithm 2.

The EPivoter algorithm is outlined in Algorithm 3. The main framework of Algorithm 3 is basically the same as that of Algorithm 2. There are two main differences. First, when obtaining an *enumerated biclique* $(P_l \cup H_l, P_r \cup H_r)$, we count the (p, q)-bicliques contained in it using a combinatorial counting method, since each subset of P_l and P_r with size $p - |H_l|$ and $q - |H_r|$ respectively can yield a different (p, q)-biclique, i.e., the number of (p, q)-bicliques is exactly equal to $\binom{|P_l|}{p-|H_l|}\binom{|P_r|}{q-|H_r|}$ (lines 11-12 and lines 17-18). Second, Algorithm 3 uses a degree-ordering based optimization technique to further improve the efficiency. The key idea of the degree-ordering technique is that for each *enumerated biclique*, there always exists an edge whose two end-vertices have the lowest ranks in terms of the degree ordering. That implies that every *enumerated biclique* can be identified by the enumeration algorithm that only considers the edges whose end-vertices with ranks no less than the lowest rank,

instead of considering all edges in the graph. Specifically, in the top recursive call of Algorithm 3, for each edge $e(u, v)$, we only need to explore the subgraph induced by the set of ordering neighbors of $e(u, v) \in E$ (by the degree ordering) to compute the count of every biclique containing u and v, instead of exploring the whole graph G (lines 1-3). Clearly, the correctness of Algorithm 3 can be guaranteed by Theorem 3.5.

THEOREM 3.7. *The worst-case time and space complexity of Algorithm 3 is* $O(|E|3^{|E_{\max}|/3})$ *and* $O(|E|+|U|+|V|+d_{\max}^2)$ *respectively, where* $|E_{\max}| = \max |\vec{N}(e)|, \forall e \in E$.

PROOF. Clearly, the algorithm takes $O(3^{|\vec{N}(e)|/3})$ to process each edge by Theorem 3.3. Thus, the total running time of the algorithm is $O(\sum_{e \in E} 3^{|\vec{N}(e)|/3})$. Since $|\vec{N}(e)| \leq |E_{\max}|, \forall e \in E$, we can easily obtain that the time complexity of Algorithm 3 is $O(|E|3^{|E_{\max}|/3})$. The number of vertices in the subgraph induced by each edge is bounded by $d_{\max}$. Thus, the space complexity of Algorithm 3 $O(|E|+|U|+|V|+d_{\max}^2)$. □

Pruning tricks for counting (p, q)-bicliques. Note that if we only need to count the (p, q)-bicliques for a given p and q (not for all p and q), we can further improve Algorithm 3. Specifically, if the recursion has parameters $|H_l| > p$ or $|H_r| > q$, we can safely terminate this recursion, because any (p, q)-biclique definitely cannot be represented by the *enumerated cliques* identified by this recursion. Similarly, if the recursion has parameters $|P_l \cup H_l \cup C_l| < p$ or $|P_r \cup H_r \cup C_r| < q$, we can also safely prune such a recursion, as it clearly cannot identify (p, q)-bicliques with the required size. Algorithm 3 can also be easily extended to count the bicliques with size constraints. We can prune the branch if $|P_l \cup H_l \cup C_l| < p$ or $|P_r \cup H_r \cup C_r| < q$ and add a preprocessing step to shrink the input graph into a (p, q)-core [20].

The choice of p and q in practice. For practical applications, the values of p and q are often not very large, because small motifs are often the building blocks of large networks [21]. For example, only the count of $(2, 2)$-bicliques is useful in measuring the *Triadic Closure* of networks [30]. In application of detecting (p, q)-biclique densest subgraph [22], both p and q are often set no larger than 5. In some cases, (p, q) can be imbalanced, i.e., the value of p and q differs. For instance, [33] shows that $(5, 10)$-bicliques and $(4, 10)$-bicliques achieve the the best performance in application of optimizing the performance of graph neural network training. As a result, we recommend to set p and q no larger than 10 for many practical applications.

Further discussions. The challenge of the biclique counting problem is that a (p, q)-biclique can be located in many maximal bicliques. Since the overlap relationships among the maximal bicliques are very complicated, it is extremely hard to apply the Inclusion-Exclusion technique to exactly derive the (p, q)-biclique counts from the maximal bicliques. To overcome this challenge, we propose an edge-pivoting based enumeration technique (i.e., Algorithm 3) that can uniquely encode each biclique, thus our technique can avoid repeatedly counting. Compared to the state-of-the-art algorithm which needs to exhaustively enumerate every (p, q)-biclique, Algorithm 3 only enumerates the large bicliques (i.e., the *enumerated bicliques*) and then count the (p, q)-bicliques in the *enumerated bicliques* using a combinatorial counting method. Since the number of *enumerated bicliques* in a bipartite graph G is often much smaller than the number of (p, q)-bicliques for relatively-large p and q, our algorithm is much more efficient than the state-of-the-art algorithm as evidenced in our experiments. Moreover, once obtaining the *enumerated bicliques*, our algorithm can compute all biclique counts for all parameters p and q, while the state-of-the-art algorithm can only obtain one count of the (p, q)-cliques for a given (p, q) pair.

It is worth mentioning that existing motif counting techniques are not suitable for counting the bicliques because those techniques (e.g., edge-based sampling technique [2]) only work well for small motifs (e.g., the size smaller than 10). Moreover, those techniques are not tailored to biclique counting, thus they are likely worse than the existing highly-optimized biclique counting technique proposed in [33]. In addition, existing maximal biclique enumeration algorithms [1, 7, 17, 38] are also not suitable for counting bicliques because these algorithms are based on enumerating vertices of only one side. The vertex-based pivoting technique in these maximal biclique enumeration algorithms is not easily adapted to count bicliques. The reason is as follows: an edge-based pivot has neighbors on each side, thus it can easily encode vertices on both two sides. However, the vertex-based pivot is located on only one side, and it cannot encode both two sides as our edge-based pivot does. To our knowledge, our edge-pivoting based technique is novel and it has not been studied previously.

4 THE ZIG-ZAG SAMPLING ALGORITHMS

Although EPivoter is much more efficient than the state-of-the-art algorithm in enumerating all bicliques, it may still be costly when handling large graphs, as it still involves an expensive backtracking biclique enumeration procedure. In this section, we develop several novel approximate algorithms based on a carefully-designed zig-zag sampling technique, which can obtain an unbiased estimator for all bicliques within polynomial time. Below, we give a new concept called h-zigzag which is crucial for devising our sampling algorithms. For convenience, in the rest of this paper, we assume without loss of generality that the vertices in each side of the bipartite graph $G = (U, V, E)$ are sorted in a non-decreasing ordering based on their degrees, i.e., $u_1 \prec_d u_2 \prec_d \cdots \prec_d u_{n_1}$ and $v_1 \prec_d v_2 \prec_d \cdots \prec_d v_{n_2}$.

Definition 4.1. Given a bipartite graph $G(U, V, E)$ and an integer h, an h-zigzag in G is an *ordered* simple path $P = \{u_{i_1}, v_{j_1}, u_{i_2}, v_{j_2}, ..., u_{i_h}, v_{j_h}\}$ that satisfies (1) its length equaling $2h - 1$, and (2) $i_1 < \cdots < i_h$ and $j_1 < \cdots < j_h$.

By Definition 4.1, an h-zigzag contains h vertices on each side of the bipartite graph, and the vertices in the h-zigzag follow the degree ordering. The following lemma establishes a relationship between the h-zigzag and the (p, q)-clique.

LEMMA 4.2. *Given a (p, q)-clique of G with $p \leq q$, it exactly contains $\binom{q}{h}$ h-zigzags, if $h = p$.*

PROOF. Clearly, the lemma holds when $p = q$. If $p < q$, we denote by (L, R) with $|L| = p$ and $|R| = q$ an arbitrary (p, q)-clique. Each h-zigzag in (L, R) must contain h vertices in both sides, since the length of the h-zigzag is equal to $2h - 1$ ($h = q$). It is easy to

see that any h vertices selected from R will form a h-zigzag. Thus, a total number of $\binom{q}{h}$ h-zigzags contained in (L, R). □

For convenience, in the rest of this section, we focus mainly on counting the (p, q)-bicliques with $p \leq q$, because the same proposed technique can also be used to count the (p, q)-bicliques with $p > q$. Let $\mathcal{H}$ be the set of all h-zigzags in G, and $\mathcal{T}$ be the set of uniform h-zigzags sampled from $\mathcal{H}$. Denote by Z_i the i-th h-zigzag in $\mathcal{T}$, where $1 \leq i \leq |\mathcal{T}|$. For each $Z_i \in \mathcal{T}$, the count of the (p, q)-bicliques in G that contain Z_i is denoted as $c_{p,q}(Z_i)$. Then, based on Lemma 4.2, we can derive the following lemma.

LEMMA 4.3. *Let Z be an h-zigzag uniformly sampled from $\mathcal{H}$. The probability of each (p, q)-biclique of G containing Z is $\binom{q}{h}/|\mathcal{H}|$, where $h = p$.*

PROOF. Since each (p, q)-biclique contains $\binom{q}{h}$ h-zigzags by Lemma 4.2, the probability of each (p, q)-biclique containing Z is $\binom{q}{h}/|\mathcal{H}|$. □

Based on Lemma 4.3, we can construct an unbiased estimator for the count of (p, q)-biclique by uniformly sampling h-zigzag in G.

THEOREM 4.4. *Denote by $\mathcal{B}_{p,q}$ the set of (p, q)-bicliques. Suppose that $\mathcal{T}$ is set of h-zigzags ($h = p$) sampled uniformly from G. Then, the unbiased estimator of the count of (p, q)-bicliques in G, denoted by $|\hat{\mathcal{B}_{p,q}}|$, is*

$$|\hat{\mathcal{B}_{p,q}}| = \frac{|\mathcal{H}| \sum_{Z \in \mathcal{T}} c_{p,q}(Z)}{|\mathcal{T}| \binom{q}{h}}. \tag{3}$$

PROOF. By definition, we can easily derive the following equality

$$\sum_{Z \in \mathcal{H}} c_{p,q}(Z) = \binom{q}{h} |\mathcal{B}_{p,q}|. \tag{4}$$

The left hand side of this equality is the sum of all (p, q)-bicliques containing every h-zigzag in G, which corresponds to $\binom{q}{h}$ times the count of (p, q)-bicliques of G (right hand side of this equality) because each (p, q)-biclique contains $\binom{q}{h}$ h-zigzags. Further, we can derive that

$$E[c_{p,q}(Z)] = \frac{\binom{q}{h} |\mathcal{B}_{p,q}|}{|\mathcal{H}|}, \tag{5}$$

where $E[c_{p,q}(Z)]$ denotes the expected number of (p, q)-cliques that containing a randomly sampled h-zigzag Z. Based on this, we have

$$\begin{aligned} E[|\hat{\mathcal{B}_{p,q}}|] =& E[\frac{|\mathcal{H}| \sum_{1 \leq i \leq |\mathcal{T}|} c_{p,q}(Z)}{|\mathcal{T}| \binom{q}{h}}] \\ =& \frac{|\mathcal{H}|}{|\mathcal{T}| \binom{q}{h}} \sum_{1 \leq i \leq |\mathcal{T}|} E[c_{p,q}(Z)] \\ =& |B_{p,q}|. \end{aligned} \tag{6}$$

□

Armed with Theorem 4.4, we can estimate the number of (p, q)-cliques by uniformly sampling h-zigzags from G. The remaining issues are: (1) how to uniformly sample h-zigzag from the graph G; and (2) how to compute the total number of h-zigzags in G. Below, we will propose a novel and efficient dynamic programming (DP) algorithm to tackle these issues.

Algorithm 4: DPCount(G, h)

```
1  Initialize dp[i][e(u,v)] = 0 and dp[1][e(u,v)] = 1 for each e(u,v) ∈ E;
2  for i = 2 to 2h − 1 do
3      foreach e(u,v) ∈ E do
4          foreach e(v,u') with u' > u do
5              dp[i][e(v,u')] ← dp[i][e(v,u')] + dp[i − 1][e(u,v)];
6      foreach e(v,u') ∈ E do
7          foreach e(u',v') with v' > v do
8              dp[i + 1][e(u',v')] ← dp[i + 1][e(u',v')] + dp[i][e(v,u')];
9      i ← i + 2;
10 return dp;
```

4.1 The DP-based zig-zag sampling algorithm

We first devise a DP algorithm to compute the total number of h-zigzags in G. Then, we will show how to transform our DP-based h-zigzag counting solution to a uniform h-zigzag sampler.

Counting the number of h-zigzags. Let $Z = \{u_1, v_1, ..., u_h, v_h\}$ be an h-zigzag in G, we have $u_i < u_{i+1}$ and $v_i < v_{i+1}$ for each $1 \leq i \leq h - 1$. Thus, the total number of h-zigzags of G can be calculated by counting the h-zigzags starting with each vertex u_i in U. Denote by $dp[i][e(u, v)]$ the number of zig-zag paths with length i starting from the edge $e(u, v)$. Then, it is easy to see that the number of h-zigzags starting from u is equal to $\sum_{v \in N(u)} dp[2h - 1][e(u, v)]$. As a result, the total number of h-zigzags in G is $\sum_{e(u,v) \in E} dp[2h - 1][e(u, v)]$.

Interestingly, we find that we can compute $dp[i][e(u, v)]$ using a dynamic programming algorithm. The key idea of our DP algorithm is that for each path Z of length i starting from $e(u, v)$, it must consist of the paths of length $i - 1$ starting from v. Thus, we have the following recursive equation

$$\begin{cases} dp[i][e(u,v)] = \sum_{u' \in N^{>u}(v)} dp[i-1][e(v,u')], \\ dp[i-1][e(v,u')] = \sum_{v' \in N^{>v}(u')} dp[i-2][e(u',v')], \\ dp[1][e(u,v)] = 1, \end{cases} \tag{7}$$

where $2 \leq i \leq 2h - 1$.

Note that in Eq. (7), the notions $dp[i][e(u, v)]$ and $dp[i][e(v, u)]$ are quite different. The notion $dp[i][e(u, v)]$ corresponds to the number of paths of length of i where i is odd number, which also denotes the count of paths starting from a certain vertex in U and ending at a certain vertex in V. The notion $dp[i][e(v, u)]$ corresponds to the number of paths of even length, in which both starting vertex and ending vertex are in U. When initializing $dp[1][e(u, v)]$ to 1 for all $e(u, v) \in E$, the others $dp[i][e(u, v)]$ and $dp[i][e(v, u)]$ for $i = 2$ to $2h - 1$ can be recursively computed by Eq. (7). Thus, the total time cost to compute the count of h-zigzags of G is $O(hd_{max}|E|)$, where d_{max} is the maximum degree in G. The detailed implementation of this DP algorithm is outlined in Algorithm 4.

Optimization technique for DPCount**.** The straightforward implementation of DPCount has $O(hd_{max}|E|)$ time complexity. Here we propose a differential-interval updating technique to further speed up DPCount. Specifically, denote by $dp[i]$ the set $\{a_1, a_2, ..., a_n\}$ where $a_j = dp[i][e_j]$. We can replace $dp[i]$ with another set $\{b_1, b_2, ..., b_n\}$ such that $b_1 = a_1$ and $b_j = a_j - a_{j-1}$ for $j = 2$ to n. Then, we have $a_j = \sum_{j' \leq j} b_{j'}$, i.e, each a_i is the sum of the prefixes of $\{b_1, b_2, ..., b_n\}$. Note that lines 4-5 (lines 7-8) can be represented as updating the values of $\{a_1, a_2, ..., a_n\}$ in an interval $[l, r]$ using the same integer w ($w = dp[i - 1][e(u, v)]$ in line 5 and $w =$

Algorithm 5: DPCount++(G, h)

1 initial $dp[1][e(u,v)] = 1$ for all $e(u,v) \in E$;
2 **for** $i = 2$ **to** $2h-1$ **do**
3 initial zeros array b with size $|E|+1$;
4 **for** $j = 1$ *to* $|E|$, $e(u,v)$ *is the* j_{th} *edge* **do**
5 l, r is the interval of edges $\{e(v,u') | u' \in N^{>u}(v)\}$;
6 $w \leftarrow dp[i-1][e(u,v)]$;
7 $b[l] \leftarrow b[l] + w$; $b[r+1] \leftarrow b[r+1] - w$;
8 $dp[i][e_1] = b[1]$;
9 **for** $j = 2$ *to* $|E|$ **do**
10 $dp[i][e_j] \leftarrow dp[i][e_{j-1}] + b[j]$;
11 initial zeros array b with size $|E|+1$;
12 **for** $j = 1$ *to* $|E|$, $e(v,u')$ *is the* j_{th} *edge* **do**
13 l, r is the interval of edges $\{e(u',v') | v' \in N^{>v}(u')\}$;
14 $w \leftarrow dp[i][e(v,u')]$;
15 $b[l] \leftarrow b[l] + w$; $b[r+1] \leftarrow b[r+1] - w$;
16 $dp[i+1][e_1] = b[1]$;
17 **for** $j = 2$ *to* $|E|$ **do**
18 $dp[i+1][e_j] \leftarrow dp[i+1][e_{j-1}] + b[j]$;
19 $i \leftarrow i + 2$;
20 **return** dp

$dp[i-1][e(v,u')]$ in line 8. If $dp[i]$ is replaced with $\{b_1, b_2, ..., b_n\}$, we only need to update b_l and b_{r+1} to $b_l + w$ and $b_{r+1} - w$, respectively. After updating, we also have $a_j = \sum_{j' \le j} b_{j'}$. Thus, the computation of lines 4-5 (lines 7-8) can be achieved in $O(1)$ time using such a differential-interval updating trick. As a result, the total time complexity of DPCount can be reduced to $O(h|E|)$. The detailed implementation is outlined in Algorithm 5.

From counting to uniformly sampling. Here we propose an efficient algorithm to uniformly sample an h-zigzag based on Algorithm 4. The key point to uniformly generate an h-zigzag from G is to determine the probability distribution for all h-zigzags in G. Interestingly, we can use the counts computed by Algorithm 4 to construct the probability distribution for all h-zigzags. Specifically, by Eq. (7), the total number of h-zigzags in G is $\sum_{e(u,v)\in E} dp[2h-1][e(u,v)]$, where $dp[2h-1][e(u,v)]$ denotes the number of h-zigzags starting from the edge $e(u,v)$. Based on this, the probability of an edge $e(u,v)$ appearing in the head of an h-zigzag Z is $\frac{dp[2h-1][e(u,v)]}{\sum_{e(u,v)\in E} dp[2h-1][e(u,v)]}$. Moreover, for the next edge in Z, it must be contained in $\{e(v,u') | u' \in N^{>u}(v)\}$. The probability of an edge $e(v,u')$ appearing as the second edge in Z, given that $e(u,v)$ is the first edge of Z, is $\frac{dp[2h-2][e(v,u')]}{dp[2h-1][e(u,v)]}$. The same method can be recursively applied to determine the probabilities of the other edges appearing in Z. Based on these probabilities, we can uniformly sample an h-zigzag from G. The detailed implementation of our sampling algorithm is given in Algorithm 6.

In Algorithm 6, it admits two parameters $h_{\max}$ and Ts, where $h_{\max}$ is the maximum length of h-zigzags to be sampled and Ts is the set of sample sizes of h-zigzags for each $h \le h_{\max}$ (i.e, $Ts[h]$ denotes the sample size of the h-zigzags). First, the algorithm makes use of DPCount to get the DP table which is used to determine the sampling probabilities (line 1). For each length h, the algorithm draws $Ts[h]$ samples by invoking the DPSampling procedure (line 6). In DPSampling, it first sets a probability distribution over all edges in E based on the dp table that can be the head edge of h-zigzags (line 10). Then, the algorithm sample a head edge for an h-zigzag Z w.r.t. this probability distribution (lines 11). For each remaining edge in Z, it uses a similar method to sample an edge by first setting the probability distribution of the edges using the dp table (lines 13-22).

Algorithm 6: Sampling h-zigzags for all $h \le h_{\max}$.

Input: A bipartite graph $G = (U, V, E)$, an array Ts and an integer $h_{\max}$.
Output: For each $h \le h_{\max}$, uniformly sampling $Ts[h]$ h-zigzags.
1 Sample$(G, Ts, h_{\max}, \text{DPCount}(G, h_{\max}))$;
2 **Procedure** Sample$(G, Ts, h_{\max}, dp)$
3 $zigzags[\,] \leftarrow \{\emptyset, \emptyset, ...\}$;
4 **for** $h = 2$ *to* $h_{\max}$ **do**
5 **for** $i = 1$ *to* $Ts[h]$ **do**
6 $Z \leftarrow$ DPSampling(h, dp);
7 $zigzags[h] \leftarrow zigzags[h] \cup \{Z\}$;
8 **return** $zigzags$;
9 **Procedure** DPSampling(h, dp)
10 Set the distribution D over the edges where $p(e(u,v)) = dp[2h-1][e(u,v)] / \sum_{e(u,v)} dp[2h-1][e(u,v)]$;
11 Sample an edge $e(u,v)$ according to D;
12 $Z \leftarrow \{e(u,v)\}$;
13 **for** $i = 2h-2$ **to** $i = 2$; **do**
14 $E' \leftarrow \{e(v,u') | u' \in N^{>u}(v)\}$;
15 Set the distribution D over E' where $p(e) = dp[i][e] / \sum_{e\in E'} dp[i][e]$;
16 Sample an edge $e(v,u')$ according to D;
17 $Z \leftarrow Z \cup \{e(v,u')\}$;
18 $E' \leftarrow \{e(u',v') | v' \in N^{>v}(u')\}$;
19 Set the distribution D over E' where $p(e) = dp[i-1][e] / \sum_{e\in E'} dp[i-1][e]$;
20 Sample an edge $e(u',v')$ according to D;
21 $Z \leftarrow Z \cup \{e(u',v')\}$;
22 $u \leftarrow u'$; $v \leftarrow v'$; $i \leftarrow i-2$;
23 **return** Z;

The procedure returns Z as a sampled h-zigzag if $2h-1$ edges have been added to Z (line 23). The following theorem shows that every h-zigzag can be uniformly sampled by Algorithm 6.

THEOREM 4.5. *Algorithm 6 uniformly samples the set of h-zigzags in G for each* $h \le h_{\max}$.

PROOF. Let $\mathcal{T}$ be the set of sampled h-zigzags. Denote by $Z = \{u_1, v_1, u_2, v_2, ..., u_h, v_h\}$ a random h-zigzag in $\mathcal{T}$. Assume that $e_1 = e(u_1, v_1)$, $e_2 = (v_1, u_2)$, ..., $e_{2h-1} = e(u_h, v_h)$. Denoted by $Pr(Z)$ the probability of Z being sampled. Then, we have

$$Pr(Z) = Pr(e_1) \prod_{2\le i\le 2h-1} Pr(e_i | e_{i-1}), \tag{8}$$

where $Pr(e_1)$ is the probability that e_1 is selected as the head edge of the sampled h-zigzag, and $Pr(e_i|e_{i-1})$ is the probability that e_i is selected in the case of e_{i-1} being sampled. Based on our algorithm, we have $Pr(e_1) = \frac{dp[2h-1][e_1]}{\sum_{e\in E} dp[2h-1][e]}$ and $Pr(e_i|e_{i-1}) = \frac{dp[2h-i][e_i]}{dp[2h-i+1][e_{i-1}]}$. Then, $Pr(Z)$ can be derived by

$$\begin{aligned} Pr(Z) &= Pr(e_1) \prod_{2\le i\le 2h-1} Pr(e_i|e_{i-1}) \\ &= \frac{dp[2h-1][e_1]}{\sum_{e\in E} dp[2h-1][e]} \prod_{2\le i\le 2h-1} \frac{dp[2h-i][e_i]}{dp[2h-i+1][e_{i-1}]} \\ &= \frac{dp[2h-1][e_1]}{\sum_{e\in E} dp[2h-1][e]} \times \frac{dp[2h-2][e_2]}{dp[2h-1][e_1]} \times \cdots \\ &\quad \times \frac{dp[2][e_{2h-2}]}{dp[3][e_{2h-3}]} \times \frac{dp[1][e_{2h-1}]}{dp[2][e_{2h-2}]} \\ &= \frac{1}{\sum_{e\in E} dp[2h-1][e]}. \end{aligned} \tag{9}$$

As a result, the probability of sampling each h-zigzag from G is the same. This completes the proof. □

The time and space complexity of Algorithm 6 is analyzed in the following theorem.

THEOREM 4.6. *The time and space complexity of Algorithm 6 is* $O(h_{\max}|E| + h_{\max}d_{\max}|\mathcal{T}|)$ *and* $O(h_{\max}|E| + |\mathcal{T}|)$*, where* $\mathcal{T}$ *is the set of all the sampled h-zigzags for all* $h \le h_{\max}$.

PROOF. It is easy to see that the time complexity of Algorithm 6 is $O(t(\text{DPCount}) + t(\text{Sample}))$, where $t(\text{DPCount})$ and $t(\text{Sample})$ are the time costs of DPCount and Sample respectively. As we analyzed before, $t(\text{DPCount})$ is bounded by $O(h_{\max}|E|)$ with the differential-interval updating technique. Then, we analyze $t(\text{Sample})$, which is mainly dominated by the sample size $|\mathcal{T}|$ and the time spent on sampling an h-zigzag from G. Note that DPSampling only takes $O(h_{\max}d_{\max})$ to sample an h-zigzag since it takes $O(d_{\max})$ time to determine which neighbor vertex (lines 16, 20) is selected. Thus, $t(\text{Sample})$ is bounded by $O(h_{\max}d_{\max})$, and the total time complexity of Algorithm 6 is bounded by $O(d_{\max}|E| + h_{\max}d_{\max}|\mathcal{T}|)$.

For the space complexity, the algorithm takes $O(h_{\max}|E|)$ space to maintain the dp table and uses $O(|\mathcal{T}|)$ to store the samples, thus the total space overhead is $O(h_{\max}|E| + |\mathcal{T}|)$. □

4.2 Biclique counts estimation via zig-zag sampling

Armed with Theorem 4.4 and Algorithm 6, we are ready to devise an estimating algorithm to approximately count the (p, q)-bicliques for all p and q. However, the method of directly estimating the (p, q)-biclique counts on the entire bipartite graph G suffers from the following two limitations. First, the space usage of the DP table dp is $O(h_{\max}|E|)$, indicating that such a method can only estimate the biclique counts when $h_{\max}$ is small on large graphs. Second, most of the regions in real-world bipartite graphs are often very sparse. When sampling h-zigzags from the entire graph, there may be many h-zigzags that are not contained in any biclique of G, thus reducing the sampling performance of the algorithm.

The ZigZag **algorithm.** To overcome these limitations, we develop a novel estimating algorithm which samples h-zigzags on the neighborhood subgraphs of G, instead of the whole graph. Our algorithm is based on the fact that any biclique that contains an edge $e(u, v)$ must be contained in the subgraph G' induced by the set of neighbors of $e(u, v)$ (including $e(u, v)$ itself). Therefore, we only need to sample h-zigzags on the *local neighborhood subgraph* G', instead of on the entire bipartite graph G, to estimate the counts of bicliques containing $e(u, v)$.

Specifically, for each $e(u, v)$, we first compute the subgraph G' of G induced by $\vec{N}(e(u, v))$. Then, we sample $(h-1)$-zigzags on G'; and we can obtain an h-zigzag of G by adding $e(u, v)$ to each of $(h-1)$-zigzag. To get a uniform h-zigzag sample, we also needs to take the count of the $(h-1)$-zigzags in G' into consideration. Specifically, by Eq. (7), for each $e(u, v) \in E$, the number of h-zigzags whose head edge is $e(u, v)$ is $dp[2h-1][e(u, v)]$, which indicates that the number of $(h-1)$-zigzags in G' (induced by $\vec{N}(e(u, v))$) is exactly $dp[2h-1][e(u, v)]$. Denote by T the total number of h-zigzags of G to be sampled. Then, for each G' induced by $\vec{N}(e)$, it needs to sample $T \times \frac{dp[2h-1][e]}{\sum_{e' \in E} dp[2h-1][e']}$ $(h-1)$-zigzags in G' to guarantee uniform h-zigzag samples. Clearly, the space usage of the algorithm is dominated by the maximum size of subgraphs induced by all $\vec{N}(e)$, which is often much smaller than the size of G. Moreover, each sampled h-zigzag must be contained in the *local neighborhood subgraph* which increases the probability that a sampled h-zigzag hits a biclique (i.e., the subgraph induced by the sampled h-zigzag is a biclique), thus improving the sampling performance. The detailed implementation is outlined in Algorithm 7.

Algorithm 7: ZigZag: Estimating all bicliques in each edges' neighborhood subgraph

Input: A bipartite graph $G = (U, V, E)$, sample size T and an integer h_{max}
Output: The approximate count of (p, q)-bicliques for all $p, q \le h_{max}$

1 Initialize ans as an $h_{max} \times h_{max}$ zeros array;
2 $G' \leftarrow$ the subgraph induced by $N^{>u}(v)$ and $N^{>v}(u)$ for each $e(u, v)$;
3 **foreach** $e(u, v) \in E$ **do**
4 $dp \leftarrow DPCount(G', h_{max} - 1)$;
5 **for** $h = 1$ *to* $h_{max} - 1$ **do**
6 $hzzCnt[h] \leftarrow hzzCnt[h] + \sum_{e \in \vec{N}(e(u,v))} dp[2h-1][e]$;
7 **foreach** $e(u, v) \in E$ **do**
8 $dp \leftarrow \text{DPCount}(G', h_{max} - 1)$;
9 **for** $h = 1$ *to* $h_{max} - 1$ **do**
10 $Hs[h] \leftarrow \sum_{e \in \vec{N}(e(u,v))} dp[2h-1][e]$;
11 $Ts[h] \leftarrow T \times Hs[h]/hzzCnt[h]$;
12 $zigzags \leftarrow \text{Sample}(G', Ts, h_{max} - 1, dp)$;
13 $c_{p-1,q-1}(Z) \leftarrow \binom{|N(L)|}{q-p}$ for each $Z = (L, R) \in zigzags[p-1]$ is a biclique;
14 $c_{p-1,q-1}(Z) \leftarrow 0$ if $Z \in zigzags[p-1]$ does not induce a biclique;
15 $ans_{p,q} \leftarrow ans_{p,q} + \frac{Hs[p-1] \sum_{Z \in zigzags[p-1]} c_{p-1,q-1}(Z)}{Ts[p-1]\binom{q-1}{p-1}}$
16 **return** ans;

Algorithm 7 uses a set of arrays ans to store the estimated counts of all (p, q)-bicliques, where $p \le h_{\max}$ and $q \le h_{\max}$, i.e., $ans[i][j]$ is the estimated count of (i, j)-bicliques (line 1). The algorithm then computes the counts of the $(h-1)$-zigzags in the subgraphs induced by each $\vec{N}(e)$, where $e \in E$ (lines 2-6). The total counts for the i-zigzags is stored in $hzzCount[i]$ for each $1 \le i \le h_{\max} - 1$ (line 6). Subsequently, the algorithm determines the sample size for each h (lines 7-11) and invokes Sample to sample desired h-zigzags (line 12). For each h-zigzag sample Z, the algorithm computes $c_{p,q}(Z)$ in Theorem 4.4 by the following method. First, if Z induces a (p, p)-biclique (we assume without loss of generality that $h = p \le q$), denoted by (L, R), then $c_{p,q}(Z) = \binom{|N(L)|}{q-p}$ (line 13), where $N(L)$ is the set of common neighbors of the vertices in L. Otherwise, we have $c_{p,q}(Z) = 0$ (line 14, in this case an h-zigzag does not hit a biclique). After that, the algorithm estimates the counts of (p, q)-bicliques for all $p, q \le h_{\max}$ based on the unbiased estimator established in Theorem 4.4 (line 15). The algorithm terminates until all *local neighborhood subgraphs* are processed.

Denote by $|E_{sum}| = \sum_{e \in E} |\vec{N}(e)|$ the total size of all subgraphs induced by $\vec{N}(e)$ for each $e \in E$. Let $|E'|$ be the maximum size among all these subgraphs. Then, the time and space complexity of Algorithm 7 is analyzed as follows.

THEOREM 4.7. *The time and space complexity of Algorithm 7 is* $O(|E_{sum}|h_{\max} + |E|h_{max}^2 + Td_{\max}h_{\max}^2)$ *and* $O(h_{\max}|E'| + |E|)$ *respectively, where* T *is the total sample size for all* $h \le h_{\max}$*, and* $d_{\max}$ *is the maximum degree of* G.

PROOF. In lines 3-6, DPCount takes $O(|\vec{N}(e)|h_{\max})$ time. Thus, the total time cost in lines 3-6 is $O(\sum_{e \in E} |\vec{N}(e)|h_{\max})$, which is bounded by $O(|E_{sum}|h_{\max})$. Similarly, in lines 8-11, the total time cost is also bounded by $O(|E_{sum}|h_{\max})$. Since each h-zigzag can be sampled in $O(h_{\max}d_{\max})$ time, the total time used for sampling is

$O(Td_{\max}h^2_{\max})$. In lines 13-14, it takes at most $O(d_{\max}h_{\max})$ time to compute the number of bicliques containing a sampled h-zigzag. Updating ans needs $O(h^2_{max})$ for each edge (line 15). As a result, the total time complexity of Algorithm 7 is $O(|E_{sum}|h_{\max} + |E|h^2_{max} + Td_{\max}h^2_{\max})$.

For the space complexity, the algorithm takes $O(|E|)$ to maintain the input bipartite graph, and uses $O(h_{\max}|E'|)$ space to maintain the dp table when processing the maximum neighborhood subgraph. Therefore, in the worst case, the space usage of Algorithm 7 is bounded by $O(h_{\max}|E'| + |E|)$. □

The ZigZag++ **algorithm.** The main limitation of Algorithm 7 is that it needs to process $O(|E|)$ neighborhood subgraphs which is often costly. To further boost the efficiency, we propose a different algorithm, called ZigZag++, that is based on sampling h-zigzags on the neighborhood subgraphs constructed by vertices, instead of induced by edges as we do in Algorithm 7. Specifically, for each vertex u, we define a *2-hop subgraph* of u as follows.

Definition 4.8 (2-hop subgraph). Given a bipartite graph $G(U, V, E)$, we refer to $G_u(U_u, V_u, E_u)$ as the 2-hop subgraph of a vertex $u \in U$ if $V_u = N(u)$, $U_u = \cup_{v\in N(u)} N^{>u}(v)$ and $E_u = \{e(u', v') \in E | u' \in U_u, v' \in V_u\}$.

Clearly, by Definition 4.8, all bicliques in G must be contained in the set of all 2-hop subgraphs. As a result, we only need to sample h-zigzags on the 2-hop subgraphs, instead of on the entire graph G, to estimate the biclique counts for all p and q. The general steps of ZigZag++ are almost the same as those of Algorithm 7, except the graph construction part. Specifically, ZigZag++ first constructs the 2-hop subgraph for each vertex $u \in U$. Then, for each 2-hop subgraph, ZigZag++ computes the counts of h-zigzags contained in it using DPCount. Similar to the lines 9-11 of ZigZag, to generate a uniform h-zigzag sample, ZigZag++ also uses the h-zigzags count in each 2-hop subgraph to determine the sample size. Then, ZigZag++ invokes Sample to sample desired h-zigzags. Likewise, based on Theorem 4.4, ZigZag++ constructs an unbiased estimator using the uniform h-zigzag samples. The pseudo code of ZigZag++ is outlined in Algorithm 8.

Let $|N_{sum}| = \sum_{u\in U} |E_u|$, where E_u is the set of edges in the 2-hop graph of u. Denote by $|E_{\max}| = \max_{u\in U} |E_u|$ is the maximum size among all 2-hop graphs. Then, the time and space complexity of ZigZag++ is shown in the following theorem.

THEOREM 4.9. *The time and space complexity of* ZigZag++ *is* $O(|N_{sum}|h_{\max} + |V|h^2_{max} + Td_{\max}h^2_{\max})$ *and* $O(h_{\max}|E_{\max}| + |E|)$ *respectively, where* T *is the total sample size for all* $h \le h_{\max}$*, and* $d_{\max}$ *is the maximum degree of* G.

PROOF. In the counting stage for h-zigzags, the time complexity of DPCount is dominated by the number of edges in each 2-hop graph. Thus, it takes a total of $O(\sum_{u\in U} |E_u|)$ time to count all h-zigzags. In the sampling stage, ZigZag++ also requires $O(Td_{\max}h^2_{\max})$ time to sample h-zigzags in all 2-hop graphs of G based on a similar analysis in Theorem 4.7. For the space complexity, ZigZag++ uses at most $O(h_{\max}|E_{\max}|)$ space to maintain the dp table, and consumes $O(|E|)$ to store the graph G. □

Algorithm 8: ZigZag++: Estimating all bicliques in each vertex's neighborhood subgraph

Input: A bipartite graph $G = (U, V, E)$, sample size T and an integer h_{max}
Output: The approximate count of (p, q)-bicliques for all $p, q \le h_{max}$

1 Initialize ans as a $h_{max} \times h_{max}$ zeros array;
2 **foreach** $u \in U$ **do**
3 $\quad U_u \leftarrow \{u\}; V_u \leftarrow N(u); E_u \leftarrow \emptyset$;
4 $\quad$ **foreach** $v \in N(u)$ **do**
5 $\quad\quad$ **foreach** $w \in N^{>u}(v)$ **do**
6 $\quad\quad\quad U_u \leftarrow U_u \cup \{w\}$;
7 $\quad\quad\quad E_u \leftarrow E_u \cup \{(w, v)\}$;
8 $\quad G_u \leftarrow G(U_u, V_u, E_u)$;
9 $\quad dp \leftarrow \text{DPCount}(G_u, h_{max})$;
10 $\quad$ **for** $h = 1$ *to* h_{max} **do**
11 $\quad\quad hzzCnt[h] \leftarrow hzzCnt[h] + \sum_{e(u,v'),v'\in N(u)} dp[2h-1][e]$;
12 **foreach** $u \in U$ **do**
13 $\quad dp \leftarrow \text{DPCount}(G_u, h_{max})$;
14 $\quad$ **for** $h = 1$ *to* h_{max} **do**
15 $\quad\quad Hs[h] \leftarrow \sum_{e(u,v'),v'\in N(u)} dp[2h-1][e]$;
16 $\quad\quad Ts[h] \leftarrow T \times Hs[h]/hzzCnt[h]$;
17 $\quad zigzags \leftarrow \text{Sample}(G_u, Ts, h_{max}, dp)$;
18 $\quad ans_{p,q} \leftarrow ans_{p,q} + \frac{Hs[p]\sum_{Z=(L,R)\in zigzags[p]} \binom{|N(L)|}{q-p}}{Ts[p]\binom{q}{p}}$ for $p \le q$;
19 $\quad ans_{p,q} \leftarrow ans_{p,q} + \frac{Hs[q]\sum_{Z=(L,R)\in zigzags[q]} \binom{|N(R)|-1}{p-q}}{Ts[q]\binom{p-1}{q-1}}$ for $p > q$;
20 **return** ans;

Comparison between ZigZag **and** ZigZag++**.** Note that ZigZag++ only needs to process $O(|U|)$ *local neighborhood subgraphs*, while ZigZag has to handle $O(|E|)$ subgraphs. Intuitively, ZigZag++ should be more efficient in terms of running time, as $|U| < |E|$. More formally, by Theorem 4.7 and Theorem 4.9, the difference in time complexity between ZigZag and ZigZag++ mainly lies in the total size of the constructed subgraphs, i.e, $O(|E_{sum}|)$ in ZigZag and $O(|N_{sum}|)$ in ZigZag++. Since $|E_{sum}| = \sum_{e\in E} |\vec{N}(e)|$ and $|N_{sum}| = \sum_{u\in U} |E_u|$, we can derive that $\sum_{e\in E} |\vec{N}(e)| = \sum_{e\in E} ce_e$ and $\sum_{u\in U} |E_u| = \sum_{e\in E} cn_e$, where ce_e and cn_e denote the number of corresponding subgraphs that contains the edge e respectively, i.e, $ce_e = |\{e' \in E | e \in \vec{N}(e')\}|$ and $cn_e = |\{u \in U | e \in E_u\}|$. It is easy to see that $ce_e = O(d^2_{\max})$ and $cn_e = O(d_{\max})$ in the worst case. This is because $e(u, v) \in \vec{N}(e'(u', v'))$ needs $u \in N^{>u'}(v'), v \in N^{>v'}(u')$ while $e(u', v) \in E_u$ only needs $v \in N(u)$. Thus, we have $\frac{|E_{sum}|}{|N_{sum}|} = \frac{O(ce_e)}{O(cn_e)} = O(d_{\max})$, which means that ZigZag++ has superiority than ZigZag by an $O(d_{\max})$ factor in time complexity.

Remark. Note that both ZigZag and ZigZag++ are designed to estimate the counts of all bicliques for all p and q. When we only need the count of a particular (p, q)-clique, it is sufficient to count and sample h-zigzags for only one $h = \min(p, q)$ in both ZigZag and ZigZag++, instead of processing all h, which can significantly improve the time and space usages of our algorithms.

4.3 Estimation accuracy analysis

In this subsection, we analyze the estimation accuracy of our sampling algorithms. Our analysis relies on the classic Hoeffding's inequalities which are shown as follows.

THEOREM 4.10. **Hoeffding's inequality [8, 12]** *For the random variables* $X_i \in [0, Z], 1 \le i \le n$*, we let* $X = \sum_{1\le i\le n} X_i$*. Then, for*

$\delta > 0$, we have

$$P(X \geq (1+\delta)E[X]) \leq \exp\left(-\frac{2\delta^2 E[X]^2}{nZ^2}\right),$$
$$P(X \leq (1-\delta)E[X]) \leq \exp\left(-\frac{2\delta^2 E[X]^2}{nZ^2}\right). \quad (10)$$

Based on Theorem 4.10, we can derive the estimation error of our algorithms as shown in the following theorem.

THEOREM 4.11. *Denote by $\rho = \frac{|\mathcal{B}|\binom{q}{h}}{|\mathcal{H}|}$ where $p < q$ and $h = p$, $\mathcal{B}$ and $\mathcal{H}$ are the sets of (p,q)-bicliques and h-zigzags of G respectively. Let $Z = \max_{1\leq i\leq T}\{c_{p,q}(Z_i)\}$, where Z_i is a sampled h-zigzag in G. Then, with probability $1-\epsilon$, both* ZigZag *and* ZigZag++ *obtain a $1-2\delta$ approximation for the count of (p,q)-biclique if $T \geq \frac{Z^2}{2\rho^2\delta^2}\ln\frac{1}{\epsilon}$, where ϵ and δ are small positive values and T is the sample size.*

PROOF. Denote by $\mathcal{T}$ the set of sampled h-zigzags of G. For the i-th h-zigzag $Z_i \in \mathcal{T}$, we call X_i the count of (p,q)-bicliques containing the h-zigzag Z_i (i.e., $X_i = c_{p,q}(Z_i)$), where $1 \leq i \leq T$. Let $\hat{\rho} = \frac{\sum_{1\leq i\leq T} X_i}{T}$. Then, we have $E[\hat{\rho}] = E[X_i] = \frac{|\mathcal{B}|\binom{q}{h}}{|\mathcal{H}|} = \rho$ (or $E[\hat{\rho}T] = \rho T$) based on Theorem 4.4. Suppose that X_i is a random variable in $[0, Z]$, and let $X = \sum_{1\leq i\leq T} X_i$, where $Z = \max_{1\leq i\leq T} c_{p,q}(Z_i)$. It can be seen that $E[X] = E[\hat{\rho}T] = \rho T$. Given a positive value δ, by Hoeffding's inequality 4.10, we then have

$$\begin{aligned} Pr(X \geq (1+\delta)E[X]) &= Pr(\hat{\rho}T \geq (1+\delta)\rho T) \\ &\leq \exp\left(-\frac{2\delta^2(\rho T)^2}{TZ^2}\right) \leq \exp\left(-\frac{2\delta^2\rho^2 T}{Z^2}\right), \\ Pr(X \leq (1-\delta)E[X]) &= Pr(\hat{\rho}T \leq (1-\delta)\rho T) \\ &\leq \exp\left(-\frac{2\delta^2(\rho T)^2}{TZ^2}\right) \leq \exp\left(-\frac{2\delta^2\rho^2 T}{Z^2}\right). \end{aligned} \quad (11)$$

Further, we have

$$Pr\left(\frac{|\hat{\rho}-\rho|}{\rho} \geq \delta\right) \leq 2\exp\left(-\frac{2\delta^2\rho^2 T}{Z^2}\right). \quad (12)$$

Let $\exp\left(-\frac{2\delta^2\rho^2 T}{Z^2}\right) \leq \epsilon$. Then, we derive that $T \geq \frac{Z^2}{2\rho^2\delta^2}\ln\frac{1}{\epsilon}$. □

In Theorem 4.11, we can observe that the sample size T is mainly determined by $(\frac{Z}{\rho})^2$, i.e., the larger $(\frac{Z}{\rho})^2$ is, the more samples T are required to ensure a high accuracy of our algorithms, where Z is a maximum value of $c_{p,q}(Z_i)$ for each $Z_i \in \mathcal{T}$. As shown in our experiments, $(\frac{Z}{\rho})^2$ is often small in most real-world bipartite graphs. Thus, the proposed algorithms generally do not require a large sample size T to achieve a good accuracy in real-world bipartite graphs as confirmed in our experiments.

Accuracy comparison between ZigZag **and** ZigZag++**.** In ZigZag, each sampled h-zigzag with the head edge $e(u,v)$ must be contained in $\vec{N}(e(u,v)) \cup \{e(u,v)\}$. However, in ZigZag++, the sampled h-zigzags with a head edge $e(u,v)$ are contained in the 2-hop graph G_u of u by Definition 4.8. By definition, the edges in G_u are not necessary the neighbor edges of $e(u,v)$, while the subgraph G' constructed in ZigZag is induced by all neighbor edges of $e(u,v)$. Intuitively, the edges in G' is closely connected to $e(u,v)$, while all edges in G_u are not necessary closely connected to $e(u,v)$. As a result, an h-zigzag sampled from G' is more likely contained in a biclique than that sampled from G_u. Therefore, for a fixed sample size, ZigZag can achieve a better estimation accuracy than ZigZag++, as confirmed in our experiments.

Discussions. For the small subgraph counting problem, existing sampling-based algorithms can be classified into two categories: (1) exponential-time algorithms [2, 4, 5, 13, 15], and (2) polynomial-time algorithms [24, 32, 35]. For the exponential-time algorithms, they either need to invoke an exponential-time procedure for sampling [4, 5, 13, 15], or need to use an exponential-time exact algorithm on the samples to compute the final results [2]. The polynomial-time algorithms are often with a theoretical guarantee based on the *pattern-hitting ratio* ρ [24, 32, 35], i.e., the ratio between the number of subgraphs (the subgraphs need to count) and the total number of *sampled patterns*. For example, for k-clique counting, [35] proposed a k-color set sampling algorithm, where the sampling performance of this algorithm depends on the ratio between the number of k-cliques and the number of k-color sets. Clearly, our h-zigzag sampling algorithms also belong to the second category, and the theoretical guarantees of our algorithms (Theorem 4.11) are very similar to that of [35]. To our knowledge, for the subgraph counting problem, no polynomial-time sampling algorithm with a theoretical guarantee independent of ρ is known. Note that for most sampling-based algorithms, the sample size is often set as a fixed value T (e.g., $T = 10^5$) in practice [13, 15, 24, 32, 35], although the sample size of the algorithm in the second category depends on the *pattern-hitting ratio* ρ. In our experiments, we will also show that our algorithms are very efficient and effective by setting the sample size $T = 10^5$.

5 THE HYBRID BICLIQUE COUNTING ALGORITHM

Intuitively, the proposed sampling-based approximation algorithms often work well when the bipartite graph is dense. This is because in a denser bipartite graph an h-zigzag is more likely to be contained in a biclique, thus resulting in better sampling performance. However, for very sparse bipartite graphs, our exact EPivoter algorithm performs well as the number of *enumerated bicliques* is often not very large when the bipartite graph is sparse. These intuitions motivate us to develop a hybrid algorithm by integrating both exact and approximation algorithms. The key idea of our hybrid algorithm is that we use the exact algorithm to compute the biclique counts only in the *sparse regions* of the bipartite graph, while apply the sampling-based algorithm to estimate the biclique counts in the *dense regions* of the bipartite graph. The remaining question is how can we partition a bipartite graph into sparse regions and dense regions? Below, we propose a heuristic approach to achieve this goal.

A heuristic bipartite graph partition strategy. Before introducing our heuristic partition strategy, we first give a definition as follows.

Definition 5.1. For each edge $e(u,v)$ in G, we define the weight of $e(u,v)$ as $w(e(u,v)) = |\vec{N}^{>u}(v)| \times |\vec{N}^{>v}(u)|$. For each vertex $u \in U$, we define the weight of u as $w(u) = \sum_{v\in N(u)} w(e(u,v))$.

Based on Definition 5.1, we present a heuristic approach to split the original bipartite graph into two regions, one of which is a sparse

Algorithm 9: Partition the bipartite graph into sparse and dense regions

Input: Degree ordered bipartite $G = (U, V, E)$ and a threshold τ
Output: The dense and sparse regions of G

1 Initialize an array deg with $deg(v) = d(v)$ for each $v \in U \cup V$;
2 **foreach** $u \in U$ **do**
3 $w(u) \leftarrow 0$;
4 **foreach** $v \in N(u)$ **do**
5 $deg(v) \leftarrow deg(v) - 1; deg(u) \leftarrow deg(u) - 1$;
6 $w(u) \leftarrow w(u) + deg(v) \times deg(u)$;
7 **if** $w(u) > \tau$ **then** $D \leftarrow D \cup \{u\}$;
8 **else** $S \leftarrow S \cup \{u\}$;
9 **return** D, S;

region and the other is a dense region. Given a threshold τ, if $w(u) > \tau$, it will be added into the dense region, otherwise it is pushed into the sparse region. We can devise a peeling algorithm to compute the weight $w(u)$ for each vertex u. The detailed implementation is shown in Algorithm 9. Suppose without loss of generality that the input bipartite graph is a degree ordered bipartite graph. The algorithm first initializes an array deg to maintain the degrees of vertices in G. Then, for each vertex $u \in U$, it computes the $w(u)$ by Definition 5.1 (lines 4-6). If $w(u) \leq \tau$, the vertex u is pushed into the sparse region, otherwise it is added into dense region (lines 7-8). Note that deg always maintains the degree of each vertex in the remaining graph of G. Thus, for each $e(u, v)$, $deg(u) \times deg(v)$ is exactly equal to $w(e(u, v))$. It is easy to show that both the time and space complexity of Algorithm 9 are $O(|E|)$.

The hybrid algorithm for counting bicliques. After obtaining the sparse region S and the dense region D of G, the hybrid algorithm invokes the exact EPivoter algorithm to compute the counts of all bicliques in the subgraph induced by the edges $\{e(u, v)|u \in S\}$ and invokes the ZigZag or ZigZag++ algorithm to estimate the counts of all bicliques in the subgraph induced by the edges $\{e(u, v)|u \in D\}$. Thanks for the degree ordering, we can ensure that each biclique is counted once by the hybrid algorithm. For implementation details, we only need to modify the line 2 in Algorithm 3 by adding a constraint $u \in S$ in the "for" loop, and modify the line 3 and line 7 in Algorithm 7 by adding a constraint $u \in D$ in the "for" loop (or modify the line 2 and line 13 in Algorithm 8 by adding a constraint $u \in D$ in the "for" loop).

Remark. Note that when we only need to count (p, q)-bicliques for a given pair (p, q), we can also use the state-of-the-art (p, q)-biclique algorithm [33] to count the (p, q)-bicliques in the subgraph induced by the edges $\{e(u, v)|u \in S\}$ (i.e., the spare region) if both p and q are not very large, because it is often very fast for small p and q given that the bipartite graph is very sparse.

6 APPLICATIONS OF BICLIQUE COUNTING

In this section, we show two applications of our (p, q)-biclique counting techniques.

Higher-order clustering coefficient. The higher-order clustering coefficient based on the k-clique counts [36, 37] is an important measurement that provides a comprehensive view of complex networks. As shown in [36], networks from the same domain typically have similar higher-order clustering coefficient characteristics. According to the definition in [36], we can easily extend such a higher-order clustering coefficient to bipartite graphs based on the (p, q)-biclique counts. Specifically, the higher-order clustering coefficient of a bipartite graph $hcc_{p,q}$ can be defined as $hcc_{p,q} \triangleq 2pq\frac{C_{p,q}}{W_{p,q}}$, where $C_{p,q}$ is (p, q)-biclique counts and $W_{p,q}$ is the count of (p, q)-*wedges*. Here a (p, q)-*wedge* is a connected non-induced subgraph which contains a $(p - 1, q)$-biclique as the core and one extra node on the left side or a $(p, q - 1)$-biclique as the core and one extra node on the right side. The extra node connects at least one node on the other side. The (p, q)-biclique is a special kind of (p, q)-wedge, namely *closed* (p, q)-*wedge*. The value of $hcc_{p,q}$ ranges from 0 to 1, which indicates the probability of a (p, q)-wedge being closed.

Note that we can compute $hcc_{p,q}$ by our biclique counting algorithms. This is because the value of $W_{p,q}$ depends on $C_{p-1,q}$ and $C_{p,q-1}$. Let v be a vertex on the left side. Denote the count of (p, q)-wedges containing v by $W_v(p, q)$ and the count of (p, q)-bicliques containing v by $C_v(p, q)$. We can derive that $W_v(p, q) = C_v(p, q - 1)(|N_v| - q + 1)$. More specifically, we can slightly modify the Count procedure in Algorithm 3 to count $W_v(p, q)$. If v is a vertex in P_l of the Count procedure, $W_v(p, q)$ is $\binom{|P_l|-1}{p-|H_l|-1}\binom{|P_r|}{q-1-|H_r|}(|N_v| - q - 1)$. Similar formulations can be derived if v is in H_l, P_r or H_r of the Count procedure. Finally, we can obtain $W_{p,q} = \sum_{v \in U \cup V} W_v(p, q)$ which is the total counts of (p, q)-wedges.

Higher-order densest subgraph mining. Finding higher-order densest subgraph based on k-cliques on traditional graphs [11, 27, 29] and based on (p, q)-bicliques on bipartite graphs [22] is an important operator for many graph analysis applications. In bipartite graphs, the (p, q)-biclique densest subgraph problem aims to identify a subgraph S with the maximum (p, q)-biclique density (denoted by $\gamma(S)$), which is defined as the ratio between the count of (p, q)-bicliques and the number of vertices in the subgraph. The exact algorithm to find the (p, q)-biclique densest subgraph is based on a parametric max-flow procedure which is often intractable for large bipartite graphs [22].

To overcome this issue, we can devise a *peeling* algorithm based on our (p, q)-biclique counting techniques, by extending the existing peeling algorithm for the k-clique densest subgraph problem [11, 29]. Specifically, our peeling algorithm iteratively removes the vertex that has the minimum (p, q)-biclique counts and record the (p, q)-biclique density of the subgraph generated in each iteration. The algorithm outputs the subgraph with the maximum (p, q)-biclique density during the peeling procedure.

Note that we can slightly modify the Count procedure in Algorithm 3 to compute the (p, q)-biclique count for each vertex (also called local count). Specifically, if v is a vertex in P_l, then the count of (p, q)-bicliques containing node v is $\binom{|P_l|-1}{p-|H_l|-1}\binom{|P_r|}{q-|H_r|}$. If v is in H_l, the count is $\binom{|P_l|}{p-|H_l|}\binom{|P_r|}{q-|H_r|}$. Similar formulations can also be derived if v is in P_r or H_r. The following theorem shows that our *peeling* algorithm can achieve a $\frac{1}{p+q}$-approximation for the (p, q)-biclique densest subgraph problem.

THEOREM 6.1. *Denote by S^* the (p, q)-biclique densest subgraph. The peeling algorithm returns a $\frac{1}{p+q}$-approximate answer $\tilde{S}$, i.e. $\gamma(\tilde{S}) \geq \frac{\gamma(S^*)}{p+q}$.*

Table 1: Datasets

Datasets	$\|U\|$	$\|V\|$	$\|E\|$	$\overline{d_U}$	$\overline{d_V}$
Github	56,519	120,867	440,237	7.8	3.6
StackOF	545,195	96,678	1,301,942	2.4	13.5
Twitter	175,214	530,418	1,890,661	10.8	3.6
IMDB	685,568	186,414	2,715,604	4.0	14.6
Actor2	303,617	896,302	3,782,463	12.5	4.2
Amazon	2,146,057	1,230,915	5,743,258	2.7	4.7
DBLP	1,953,085	5,624,219	12,282,059	6.3	2.2

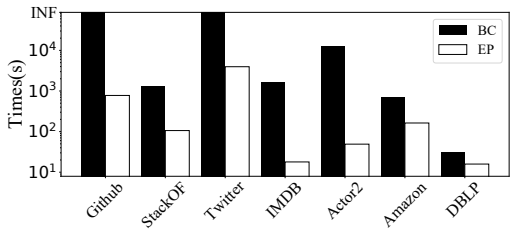

Figure 4: Runtime of different exact biclique counting algorithms for all pairs of (p, q)

PROOF. Since S^* is the (p, q)-biclique densest subgraph, we have $\gamma(S^*) \geq \gamma(S^* \setminus \{v\})$. Denote by $c(S^*)$ the total counts of S^* and $c_v(S^*)$ is the local count of v in S^*. Then, we have $\frac{c_(S^*)}{|S^*|} \geq \frac{c(S^*)-c_v(S^*)}{|S^*|-1}$. Further, we can derive that $c_v(S^*) \geq \frac{c(S^*)}{|S^*|} = \gamma(S^*)$. Let v be the vertex satisfying $v \in S^*$ and $\forall u \in S^*, u \in S_v$ where S_v is the suffix of the peeling sequence starting at v. Then, we have $S^* \subset S_v$ and $c_v(S_v) \geq c_v(S^*)$. After that, we have

$$\gamma(S_v) = \frac{c(S_v)}{|S_v|} = \frac{\sum_{u \in S_v} c_u(S_v)}{(p+q)|S_v|} \geq \frac{\sum_{u \in S_v} c_u(S^*)}{(p+q)|S_v|} \geq \frac{\sum_{u \in S_v} \gamma(S^*)}{(p+q)|S_v|} = \frac{\gamma(S^*)}{p+q}. \quad (13)$$

□

7 EXPERIMENTS

In this section, we conduct extensive experiments to evaluate the proposed algorithms. For exact biclique counting, we implement the EP algorithm which is our edge-pivot based algorithm proposed in Algorithm 3. We use the state-of-the-art algorithm [33], denoted by BC, as the baseline algorithm. Since BC can only count the (p, q)-bicliques for a specific pair of (p, q), we run BC in multiple times by varying p and q to get the counts of (p, q)-bicliques for all pairs of (p, q). In our experiments, we will also compare our algorithms with BC to count (p, q)-cliques with only one pair of (p, q), although we focus mainly on counting all (p, q)-bicliques for all pairs of (p, q).

For approximate biclique counting, we implement five different algorithms: ZZ, ZZ++, EP/ZZ, EP/ZZ++ and PSA [2]. Here ZZ and ZZ++ are the proposed ZigZag and ZigZag++ algorithm developed in Section 4. Both EP/ZZ and EP/ZZ++ are the hybrid algorithms proposed in Section 5, which integrate both exact and sampling-based counting techniques. More specifically, EP/ZZ is a hybrid algorithm integrating both EP and ZZ, and EP/ZZ++ combines both EP and ZZ++. All approximate algorithms have two parameters: the maximum h-zigzag size $h_{\max}$ and the sample size T. In our experiments, we set $h_{\max} = 10$ and $T = 10^5$ as default values. Unless otherwise specified, when varying one parameter, the other parameters are set to their default value. PSA is a general subgraph counting algorithm, which first samples a set of edges using a priority sampling technique and then enumerates the (p, q)-bicliques in the graph induced by the set of sampled edges using the state-of-the-art BC algorithm [33]. We use the count of $(2, 2)$-biclique as the weight of edge for priority sampling as suggested in [2] and set the sample size as $T \times h_{max}$ for a fair comparison. We will also study how these parameters affect the performance of different algorithms. For all approximate algorithms, the results in the experiments are the average results over 20 runs. All algorithms are implemented in C++. We evaluate all algorithms on a server with an AMD 3990X CPU and 256GB memory running linux CentOS 7 operating system.

We use 7 large real-world bipartite graphs in our experiments. The detailed statistics of our datasets are summarized in Table 1, where the last two columns $\overline{d_U}$ and $\overline{d_V}$ correspond to the average degree of the upper-side and lower-side vertices, respectively. All datasets are downloaded from http://konect.cc/.

7.1 Results of counting all bicliques

Runtime of different algorithms. We first compare two exact algorithms EP and BC to count all bicliques for all pairs of (p, q). We use the symbol "INF" to represent that the algorithm cannot terminate within 24 hours. The results on all datasets are shown in Fig. 4. As can be seen, EP can be up to more than two orders of magnitude faster than BC on all datasets. For example, on Actor2, BC takes 12,476 seconds, while EP only consumes 49 seconds to count all bicliques. Moreover, we can clearly see that BC is intractable on Github and Twitter, while our algorithm still works well on these datasets. These results demonstrate the high efficiency of our EP algorithm for counting all bicliques.

Second, we compare the runtime of all algorithms given that $h_{\max} = \min\{p, q\} \leq 10$. We set $h_{\max} = 10$ based on the following reasons. First, small biclique counts may be more useful for real-world applications [33]. Second, the baseline algorithm BC is often intractable when $h_{\max}$ is large. Third, our sampling-based algorithms may be not very accurate for a very large $h_{\max}$. As a result, it is more useful to compare the performance of different algorithms when $h_{\max}$ is not very large. Fig. 5 shows the results on all datasets. As can be seen, all our algorithms are substantially faster than the state-of-the-art algorithm BC to count all (p, q)-bicliques for all $p, q \leq h_{\max}$ on all datasets. When comparing ZZ and ZZ++, we find that on large graphs ZZ++ is faster than ZZ, while on small graphs ZZ is more efficient. In general, our four sampling-based algorithms are significantly faster than our exact algorithm. For example, on Actor2, EP takes 45 seconds, while ZZ, ZZ++, EP/ZZ, and EP/ZZ++ consumes 18 seconds, 15 seconds, 20 seconds, and 18 seconds respectively. These results suggest that our sampling-based algorithms are very efficient to estimate the (p, q)-bicliques for all $p, q \leq h_{\max}$ given that $h_{\max}$ is not very large.

Comparison of our sampling algorithms with PSA. Here we compare the performance of our sampling algorithms with the priority sampling based algorithm PSA. The results on DBLP is shown in Table 2. Similar results can also be observed on the other datasets. As can be seen, our sampling algorithms significantly outperform PSA in terms of both running time and estimation accuracy. When $p = q$,

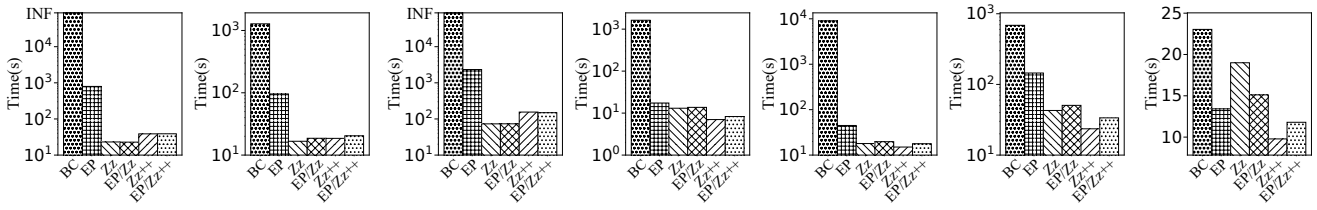

(a) Github (b) StackOF (c) Twitter (d) IMDB (e) Actor2 (f) Amazon (g) DBLP

Figure 5: Runtime of different biclique counting algorithms for all $p, q \leq h_{\max}$ ($h_{\max} = 10, T = 10^5$).

Table 2: Comparison of different sampling algorithms on DBLP **(Time (seconds), Error (%))**

Algorithms	(2, 5)		(5, 5)		all $p = q < 10$		all ($< 10, < 10$)	
	Time	Error	Time	Error	Time	Error	Time	Error
ZZ	15.02	0.01	21.81	0.02	15.28	0.06	17.93	0.14
ZZ++	7.14	0.03	26.13	1.76	8.65	0.07	9.80	0.49
EP/ZZ	12.40	0.00	8.01	0.00	13.54	0.06	15.66	0.15
EP/ZZ++	8.79	0.02	8.80	0.22	10.58	0.06	12.17	0.17
PSA	INF	-	9.79	15.01	50.73	12.52	INF	-

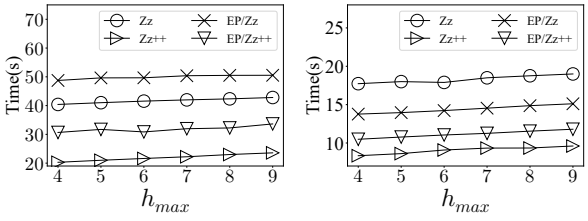

(a) Amazon (b) DBLP

Figure 6: Runtime of different approximate algorithms with varying $h_{\max}$

PSA achieves 15.01% error to count the $(5, 5)$-biclique and 12.52% average error for all $p = q < 10$, using 9.79 seconds and 50.73 seconds respectively. Our best algorithm, however, achieves near 0% error to count $(5, 5)$-biclique and 0.06% average error for all $p = q < 10$, using 8.01 seconds and 10.58 seconds respectively. When counting $(2, 5)$-biclique, PSA cannot terminate within 1 day. This is because there are 3×10^{11} $(2, 5)$-bicliques in the sampled graph and it is very costly to enumerate all of them using BC. Generally, the count of imbalanced biclique is very large (as shown in Fig. 1) even in the subgraph induced by the set of sampled edges. For the same reason, PSA cannot count (p, q)-bicliques for all $p < 10, q < 10$. The results further demonstrates the efficiency and superiority of our algorithms.

The effect of the parameter $h_{\max}$. Fig. 6 shows the runtime of four sampling-based algorithms with varying $h_{\max}$ on Amazon and DBLP, where the sample size T is set to 10^5. The results on the other datasets are consistent. As expected, the runtime of all sampling-based algorithms slightly increases with $h_{\max}$ increases. This is because the time complexity of sampling-based algorithms is insensitive w.r.t. the parameter $h_{\max}$ if $h_{\max}$ is small. Moreover, we can see that ZZ++ is much faster than ZZ with all parameters, which further confirms our analysis in Section 4.2.

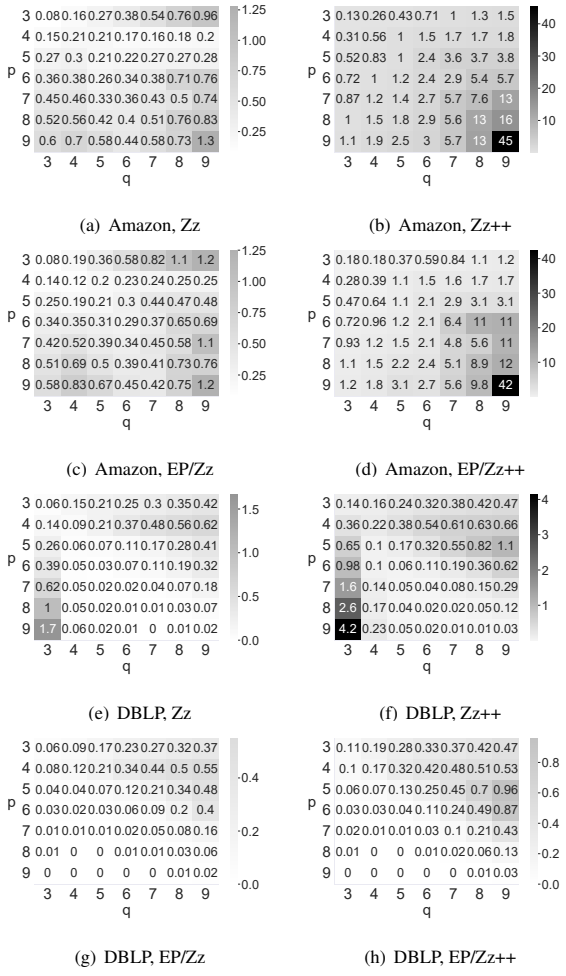

(a) Amazon, Zz (b) Amazon, Zz++ (c) Amazon, EP/Zz (d) Amazon, EP/Zz++ (e) DBLP, Zz (f) DBLP, Zz++ (g) DBLP, EP/Zz (h) DBLP, EP/Zz++

Figure 7: The heat-map of estimation errors of various algorithms with varying p and q (%).

Let $|\mathcal{B}|$ and $|\hat{\mathcal{B}}|$ be the exact and approximate counts of (p, q)-biclique respectively. The estimation error ratio of the sampling-based algorithm is defined as $\frac{||\mathcal{B}|-|\hat{\mathcal{B}}||}{|\mathcal{B}|}$. Note that when varying $h_{\max}$, the sampling-based algorithms can estimate the counts of the (p, q)-bicliques for all pairs of (p, q) with $\min\{p, q\} = h_{\max}$. Fig. 7 plots the heat-maps of the error ratios of different algorithms with varying p and q (i.e., varying $h_{\max}$ for $p, q \leq h_{\max}$) on Amazon and DBLP. Similar results can also be observed on the other datasets. From Fig. 7, we can see that all our sampling-based algorithms are

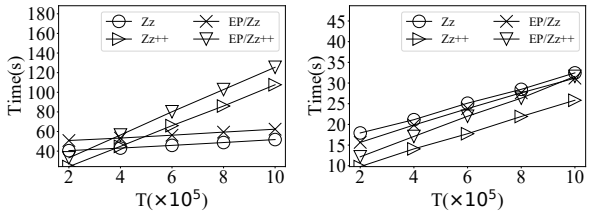

(a) Amazon (b) DBLP

Figure 8: Runtime of different approximate algorithms with various sample size

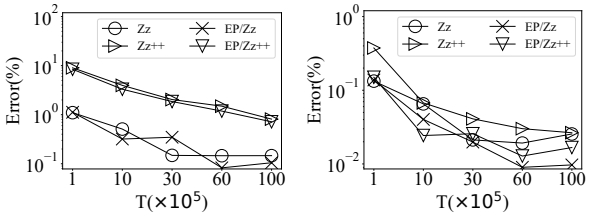

(a) Amazon (b) DBLP

Figure 9: Estimation errors of different algorithms with various T

very accurate if p and q are small (i.e., $p \leq 6$ and $q \leq 6$). Moreover, ZZ is generally more accurate than ZZ++ under most parameter settings, which is consistent with our analysis in Section 4.3. In addition, the hybrid algorithms are often much more accurate than their corresponding *pure* sampling-based algorithms. For example, on DBLP, the maximum error ratio of ZZ++ is 4.2%, while the maximum error ratio of EP/ZZ++ is 0.96%. This result indicates that our hybrid framework is indeed very powerful to improve the accuracy of the sampling-based algorithm. In general, with the increase of p or q, the error ratios of all sampling-based algorithms also increase. This is because with $h_{\max} = \min\{p, q\}$ increases, the probability of an h-zigzag contained in a biclique will be decreases, thus reducing the sampling performance.

The effect of the parameter T. Here we study the performance of our approximate algorithms with a varying sample size T. Fig. 8 shows the runtime of four approximate algorithms with varying T on Amazon and DBLP. The results on the other datasets are consistent. As expected, the runtime of all algorithms increases as T increases. Also, we can observe that ZZ++ is significantly faster than the other algorithms with varying T, which is consistent with our previous results.

Fig. 9 shows the average error ratios of our approximate algorithms with varying T on Amazon and DBLP ($h_{\max} = 10$). As shown in Fig. 9, the error ratios of all algorithms decrease as T increases. In general, ZZ has a lower error ratio than ZZ++, which further confirms our analysis in Section 4.3. Additionally, we can clearly see that EP/ZZ (EP/ZZ++) achieves a lower error ratio than ZZ (ZZ++).

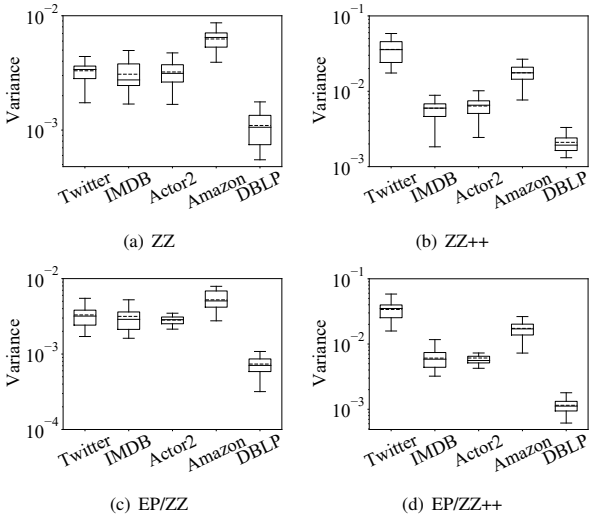

(a) ZZ (b) ZZ++

(c) EP/ZZ (d) EP/ZZ++

Figure 10: Variance of different approximate algorithms ($p \leq 6, q \leq 6, T = 10^5$)

This result further indicates that our hybrid framework can indeed improve the estimation accuracy of the sampling-based algorithms.

Variance of the approximate algorithms. Fig. 10 shows a box-diagram for the variance of each sampling-based algorithm with $p \leq 6, q \leq 6$ and $T = 10^5$ on fix datasets. The results on the other datasets and with other parameter settings are consistent. In each box-diagram, the top and bottom lines outside the box indicate the maximum and minimum values, while the solid and dashed lines in the box denote the median and mean values. As can be seen, the difference between the maximum error ratio and the minimum error ratio for each algorithm is consistently kept within a small interval, indicating that our sampling-based algorithms have small variances. Moreover, when integrated with the exact enumeration techniques, the variances of the sampling-based algorithms can further be reduced.

7.2 Results of counting (p, q)-bicliques

Runtime of different algorithms. Table 3 reports the runtime of various algorithms for specific p and q on graph Github and DBLP. The general results on other datasets are consistent. As can be seen, on Github, all our algorithms are substantially faster than BC. In general, the running time of EP is relatively stable on both Github and DBLP when varying p and q, and our sampling-based algorithms are faster than EP. On Github, ZZ++ achieves the lowest runtime which is up to three orders of magnitude faster than the baseline algorithm BC. For example, when $p = q = 9$, ZZ++ only takes 3.04 seconds to count the $(9, 9)$-bicliques, while BC consumes 3679.47 seconds. On DBLP, however, all algorithms are very efficient, and BC significantly outperforms our algorithms. The reasons may be that DBLP is very sparse and the number of bicliques contained in DBLP is relatively smaller compared to the other datasets. These results indicate that when p and q are very small and the bipartite graph does not contain too many (p, q)-bicliques, BC is the fastest, while for the other cases, our algorithms are much better.

Table 3: Runtime of different (p,q)-biclique counting algorithm for only a pair of (p,q) ($p<10, q<10$, $T=10^5$)

(p,q)	BC		EP		Zz		Zz++		EP/Zz		EP/Zz++	
	Github	DBLP	Github	DBLP	Github	DBLP	Github	DBLP	Github	DBLP	Github	DBLP
(2,3)	**1.48**	**0.48**	232.59	9.66	12.65	14.33	7.43	7.17	12.66	12.20	7.62	8.57
(2,8)	**0.35**	**0.13**	230.71	10.62	12.64	14.23	7.43	6.73	12.68	13.31	7.68	9.71
(3,4)	58.35	**0.31**	424.20	9.89	13.56	12.96	**4.91**	7.22	13.56	12.05	4.92	8.79
(3,5)	34.68	**0.21**	416.62	10.49	13.55	13.49	**4.90**	6.81	13.78	12.31	4.94	9.10
(3,9)	7.57	**0.10**	426.35	11.30	13.56	13.36	**4.92**	7.47	13.58	12.54	4.94	9.31
(4,5)	992.63	**0.28**	445.69	10.79	17.25	13.00	**1.97**	7.08	17.12	12.32	2.00	9.19
(4,8)	155.84	**0.08**	452.51	11.88	14.38	13.10	**4.78**	6.71	14.38	12.96	4.79	9.74
(5,3)	14.01	**0.04**	422.63	10.62	17.31	21.10	**4.55**	25.43	17.50	6.99	4.62	7.78
(5,6)	6049.24	**0.02**	451.07	11.98	18.11	13.51	**2.19**	6.66	17.97	12.72	2.23	9.60
(5,9)	561.67	**0.01**	462.02	13.50	15.18	14.06	5.27	7.11	15.21	13.59	**5.26**	10.46
(6,4)	148.17	**0.01**	491.63	11.12	17.51	19.04	**2.27**	28.10	17.41	7.45	2.31	8.23
(6,7)	13114.24	**0.02**	460.14	13.35	18.96	21.29	**2.42**	27.84	18.81	9.42	2.49	10.20
(7,4)	103.46	**0.01**	448.80	11.93	17.47	21.10	**2.27**	25.68	17.58	7.70	2.33	8.48
(7,7)	7728.14	**0.16**	459.96	13.90	19.61	19.29	**2.64**	28.21	19.42	9.06	2.69	9.84
(8,4)	75.52	**0.00**	450.83	12.33	17.55	18.86	**2.27**	24.88	17.39	8.28	2.33	9.08
(8,8)	6250.31	**0.07**	471.58	15.58	20.19	19.05	**2.84**	26.33	20.02	9.82	2.92	10.61
(9,4)	56.77	**0.00**	457.24	12.78	17.48	21.23	**2.27**	26.21	17.43	8.52	2.35	9.30
(9,9)	3679.47	**0.12**	480.95	16.57	20.70	18.10	**3.04**	27.02	20.54	11.02	3.13	11.79

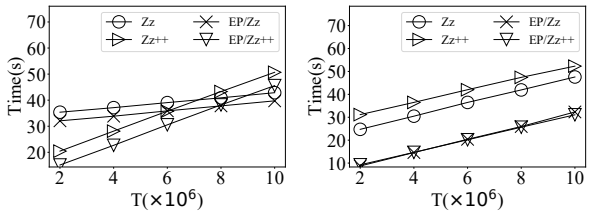

(a) Amazon (b) DBLP

Figure 11: Runtime of different approximate (p,q)-biclique counting algorithms with varying T ($p=9, q=9$).

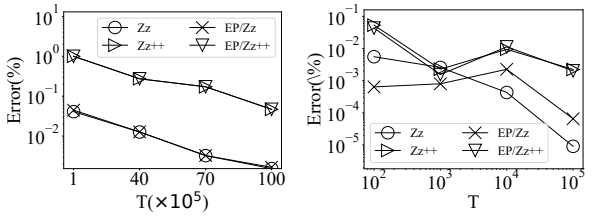

(a) Amazon (b) DBLP

Figure 12: Estimation errors of different approximate (p,q)-biclique counting algorithms with varying T ($p=9, q=9$)

The effect of parameter T. Fig. 11 and Fig. 12 respectively show the runtime and estimation errors of different approximate (p,q)-biclique counting algorithms with varying T on Amazon amd DBLP given that $p=q=9$. Similar results can also be observed on the other datasets. From Fig. 11, we can observe that the runtime of different algorithms increases as T increases, which is consistent with the results shown in Fig 8. In general, the estimation errors of our algorithms decrease when T increases. In addition, we can see that ZZ is more accurate than ZZ++, which further confirms our analysis in Section 4.3. Moreover, we can observe that the accuracy of ZZ or ZZ++ often can be further improved when integrating both the exact and sampling-based techniques. This result are consistent with our analysis in Section 5.

Table 4: The value of $\frac{Z^2}{\rho^2}$ with varying p, q (Amazon)

(p,q)	Zz	Zz++	EP/Zz	EP/Zz++
(2, 3)	3.45e+02	1.08e+02	2.94e+02	**7.69e+01**
(2, 8)	1.65e+04	5.15e+03	1.40e+04	**3.68e+03**
(3, 4)	8.73e+02	1.88e+03	**8.57e+02**	1.79e+03
(3, 5)	8.25e+03	1.77e+04	**8.10e+03**	1.69e+04
(3, 9)	1.40e+05	3.00e+05	**1.37e+05**	2.85e+05
(4, 5)	2.52e+03	6.01e+04	**2.51e+03**	5.98e+04
(4, 8)	1.04e+04	2.49e+05	**1.04e+04**	2.48e+05
(5, 3)	3.01e+03	6.48e+03	**2.96e+03**	6.17e+03
(5, 6)	4.69e+03	1.20e+06	**4.68e+03**	1.20e+06
(5, 9)	1.31e+04	3.34e+06	**1.31e+04**	3.34e+06
(6, 4)	2.44e+03	5.82e+04	**2.43e+03**	5.80e+04
(6, 7)	2.13e+04	5.32e+07	**2.13e+04**	5.32e+07
(7, 4)	6.49e+03	1.55e+05	**6.48e+03**	1.54e+05
(7, 7)	1.08e+03	2.44e+07	**1.08e+03**	2.44e+07
(8, 4)	1.33e+04	3.18e+05	**1.33e+04**	3.16e+05
(8, 8)	4.95e+03	1.04e+09	**4.95e+03**	1.04e+09
(9, 4)	2.24e+04	5.34e+05	**2.23e+04**	5.32e+05
(9, 9)	3.32e+04	8.01e+10	**3.32e+04**	8.01e+10

The value of $\frac{Z^2}{\rho^2}$. Theorem 4.11 shows that the sample size T depends on $\frac{Z^2}{\rho^2}$, where $Z=\max_{X\in H} c(X)$ and $\rho=\binom{max(p,q)}{min(p,q)}|\mathcal{B}|/|\mathcal{H}|$. Since it is very costly to compute $c(X)$ for each h-zigzag X of G, we sample a set of h-zigzags $\mathcal{H}'$ and use $\hat{Z}=max_{X\in\mathcal{H}'}c(X)$ as an estimation of Z. Table 4 reports the results of $\frac{Z^2}{\rho^2}$ on Amazon with varying p and q. As can be seen, the value of $\frac{Z^2}{\rho^2}$ in ZZ is smaller than that of ZZ++, especially when p and q is large. When integrating our exact counting technique, the value of $\frac{Z^2}{\rho^2}$ in each sampling-based algorithm decreases for all p and q, which confirms the analysis in Section 5. In addition, with the increase of p and q, the value of $\frac{Z^2}{\rho^2}$ also increases, which means that it is more difficult to estimate the count of (p,q)-bicliques for larger p and q.

Estimation error of ZZ with various ρ. Here we study the accuracy of our ZZ algorithm with various ρ. To this end, we first generate 100 random bipartite graphs with various edge densities by the classic Erdos-Renyi random graph model. Then, we use ZZ to estimate

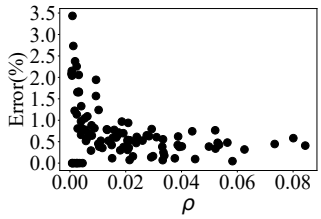

Figure 13: Estimation errors of ZZ with various ρ.

the (p, q)-biclique counts on these random bipartite graphs. Fig. 13 shows a scatter-plot on estimation error of $(4, 4)$-biclique versus ρ. The results for estimating other small (p, q)-bicliques are consistent. From Fig. 13, we can see that our algorithm performs very well even when ρ is very small. For example, even when $\rho \leq 0.02$, the estimation errors of ZZ are still less than 4% on most random bipartite graphs. This result further confirms the high efficiency of our algorithm.

Table 5: Results of the graph partition strategy

Networks	Sparse		Dense	
	$\|S\|$	$(2,2)$	$\|D\|$	$(2,2)$
Github	48,169	5.09e+05	8,350	5.04e+07
StackOF	533,949	8.62e+05	11,246	1.74e+07
Twitter	92,985	2.01e+06	82,229	2.04e+08
IMDB	654,744	1.81e+06	30,824	9.99e+06
Actor2	224,383	3.46e+06	79,234	1.96e+07
Amazon	2,108,102	2.71e+06	37,955	3.31e+07
DBLP	1,929,341	1.47e+07	23,744	1.70e+07

Evaluation of the graph partition strategy. Table 5 shows the size of the sparse region and dense region divided by Algorithm 9, as well as the count of $(2, 2)$-bicliques in each region on all datasets. The counts of (p, q)-bicliques for other p and q are consistent. From Table 5, we can clearly see that the sparse region occupies a large part of the entire graph, but it contains a very small portion of $(2, 2)$-bicliques on most datasets. The results indicate that our heuristic graph partition strategy is indeed very effective for partitioning the bipartite graph into sparse and dense regions.

7.3 Applications of (p, q)-biclique counting

Higher-order clustering coefficient. In this experiment, we use 12 real-life datasets (downloaded from http://konect.cc/) selected from four different domains. We plot the $hcc_{p,q}$ and the total running time for all pairs of (p, q) with $p = q < 10$ in Fig. 14. We can see that the higher-order clustering coefficient of the datasets in the same domain have similar distributions, which is also consistent with the results in [36] for traditional graphs. The $hcc_{p,q}$ in the first three columns varies by orders of magnitude with varying p and q. However, the changes in the authorship networks (the fourth column) are all within the same order of magnitude. These results indicate that the higher-order clustering coefficient can characterize the internal nature of the data. Moreover, by observing the running time in Fig. 14, we can clearly see that our biclique counting algorithm is

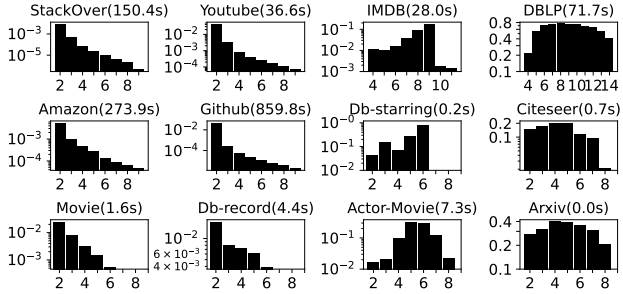

Figure 14: The y-axis is the value of $hcc_{p,q}$. The x-axis is the value of p and q. The three networks in each column are from the same domain and they share similar properties. The four columns are user-rating, user-group, actor-movie and authorship networks respectively.

Table 6: Results of finding the (p, q)-biclique densest subgraph

Networks	(p,q)	$C_{p,q}$	Time (s)		Density	
			peeling	exact	peeling	exact
Dbpedia	$(2,2)$	1.1e+06	6.7e+01	1.8e+02	249.33	249.63
Dbpedia	$(5,5)$	2.9e+03	6.6e-01	1.6e+00	105.37	105.37
IMDB	$(2,2)$	1.2e+07	7.2e+01	4.2e+03	2638.01	2638.01
IMDB	$(5,5)$	1.8e+09	1.4e+01	INF	1.4e+07	-
Amazon	$(2,2)$	3.6e+07	6.0e+02	3.5e+04	2383.19	2383.42
Amazon	$(5,5)$	6.6e+08	1.0e+02	INF	4.7e+06	-
DBLP	$(2,2)$	3.2e+07	7.9e+03	INF	6.6e+02	-
DBLP	$(5,5)$	1.3e+08	6.1e+00	INF	2.2e+06	-

very efficient to compute $hcc_{p,q}$. These results confirm the efficiency and effectiveness of our solutions.

Finding the (p, q)-biclique densest subgraph. We compare our peeling algorithm and the exact algorithm [22] to identify the (p, q)-biclique densest subgraph. Table 6 shows the results, where "INF" means that the algorithm runs out of memory. As can be seen, the result quality obtained by our peeling algorithm is almost the same as that returned by the exact algorithm. However, the running time of our peeling algorithm is at least one order of magnitude faster than the exact algorithm on most datasets. The exact algorithm is intractable on many datasets, since it needs to construct a flow network based on all (p, q)-bicliques. For example, on IMDB, when $p = q = 2$, our algorithm takes 72 seconds, while the exact algorithm consumes 4200 seconds. These results indicate that the proposed peeling algorithm, which is based on our biclique counting technique, is indeed very efficient and effective for mining the higher-order densest subgraph in bipartite graphs.

8 RELATED WORK

***K*-clique counting.** Our work is closely related to the k-clique counting problem in traditional graphs. The first exact k-clique counting (or listing) algorithm was proposed in [9] based on a backtracking enumeration technique. Such an algorithm is recently optimized by using ordering-based techniques, including the degeneracy ordering optimization proposed by Danisch et al. [10], and the color ordering optimization developed by Li et al. [18]. All these algorithms are enumeration based algorithms, thus they only work well when k is small.

To improve the efficiency, Jain and Seshadhri [14] developed an elegant algorithm, called PIVOTER, based on the pivoting technique for maximal clique enumeration [6, 28]. The PIVOTER algorithm can count the k-cliques for all k using a combinatorial counting technique, instead of exhaustively enumerating all k-cliques, thus it is substantially more efficient than all the enumeration-based algorithms. However, PIVOTER may also be very costly when processing large dense graphs [14]. To overcome this limitation, sampling-based solutions are also proposed. The state-of-the-art sampling based algorithms include the TuranShadow algorithm [13] and its improved version [15] proposed by Jain and Seshadhri, as well as the color-based sampling algorithm developed by Ye et al. [35]. All these sampling-based algorithms, however, also perform poorly when k is large. It is worth mentioning that there exist many other sampling-based algorithms for counting small subgraphs [3, 4, 16, 24, 32]. All of these algorithms were shown to be less efficient than the TuranShadow algorithm [13, 15] and the color-based sampling algorithm [35] for counting k-cliques. Unlike all these studies, our work focuses mainly on counting bicliques in bipartite graph, and all the previous techniques cannot be directly extended to handle our problems.

Subgraph enumeration in bipartite graphs. Our work is also closely related to the small subgraph enumeration problem in bipartite graphs. A notable small subgraph in bipartite graphs, called butterfly (also called $(2, 2)$-biclique), has attracted much attention in recent years. There are many advanced techniques that have been proposed to enumerate (or count) all butterflies in a bipartite graph, including both exact algorithms [25, 30, 31, 33, 40] and sampling-based approximation algorithms [19, 25, 26, 40]. Recently, another type of small subgraph in bipartite graphs, called bi-triangle or called 6-cycle, was introduced in [34], and a wedge-based algorithm for listing all bi-triangles was also proposed in [34]. In addition to small subgraph enumeration, the problem of enumerating maximal bicliques in bipartite graphs is also widely studied in recent years. One impressive work is the iMBEA algorithm developed by Zhang et al. [39] which is mainly based on a set enumeration tree technique. Abidi et al. [1] introduced a vertex-based pivoting technique, namely PMBEA, to solve this problem. Their pivoting technique, however, needs to construct a set containment DAG (directed acyclic graph) among all vertices' neighbor-sets, which is often costly in large graphs. Chen et al. [7] further presented an algorithm called ooMBEA to speed up the enumeration of iMBEA with a total search order optimization. In this work, we develop a novel edge-pivoting technique that can also be used for maximal biclique enumeration, although we focus mainly on using the edge-pivoting technique for biclique counting.

9 CONCLUSION

In this paper, we systematically investigate the problem of counting (p, q)-bicliques in a bipartite graph. We first propose an exact biclique counting algorithm, called EPivoter, based on a novel edge-pivoting technique. Then, we also propose two approximate algorithms, called ZigZag and ZigZag++, based on a novel dynamic programming based h-zigzag sampling technique. To further improve the efficiency, we develop a hybrid algorithm which applies EPivoter (ZigZag or ZigZag++) to count the bicliques on the sparse regions (dense regions) of the bipartite graph based on a carefully-designed graph partition strategy. A nice feature of all our algorithms is that they can count the (p, q)-bicliques for all pairs of (p, q), while previous algorithms are mainly tailored to count the (p, q)-bicliques with only one pair of (p, q). Extensive experiments on 7 real-life bipartite graphs demonstrate the high efficiency of the proposed solutions.

REFERENCES

[1] Aman Abidi, Rui Zhou, Lu Chen, and Chengfei Liu. 2020. Pivot-based Maximal Biclique Enumeration. In *IJCAI*.

[2] Nesreen K. Ahmed, Nick G. Duffield, Theodore L. Willke, and Ryan A. Rossi. 2017. On Sampling from Massive Graph Streams. *Proc. VLDB Endow.* 10, 11 (2017), 1430–1441.

[3] Noga Alon, Raphael Yuster, and Uri Zwick. 1994. Color-coding: a new method for finding simple paths, cycles and other small subgraphs within large graphs. In *STOC*.

[4] Marco Bressan, Flavio Chierichetti, Ravi Kumar, Stefano Leucci, and Alessandro Panconesi. 2018. Motif Counting Beyond Five Nodes. *ACM Trans. Knowl. Discov. Data* 12, 4 (2018), 48:1–48:25.

[5] Marco Bressan, Stefano Leucci, and Alessandro Panconesi. 2019. Motivo: Fast Motif Counting via Succinct Color Coding and Adaptive Sampling. *Proc. VLDB Endow.* 12, 11 (2019), 1651–1663.

[6] Coenraad Bron and Joep Kerbosch. 1973. Finding All Cliques of an Undirected Graph (Algorithm 457). *Commun. ACM* 16, 9 (1973), 575–576.

[7] Lu Chen, Chengfei Liu, Rui Zhou, Jiajie Xu, and Jianxin Li. 2022. Efficient Maximal Biclique Enumeration for Large Sparse Bipartite Graphs. *Proc. VLDB Endow.* 15, 8 (2022), 1559–1571.

[8] H. Chernoff. 1952. A Measure of Asymptotic Efficiency for Tests of a Hypothesis Based on the sum of Observations. *Annals of Mathematical Statistics* 23, 4 (1952), 493–507.

[9] Norishige Chiba and Takao Nishizeki. 1985. Arboricity and Subgraph Listing Algorithms. *SIAM J. Comput.* 14, 1 (1985), 210–223.

[10] Maximilien Danisch, Oana Balalau, and Mauro Sozio. 2018. Listing k-cliques in Sparse Real-World Graphs. In *WWW*.

[11] Yixiang Fang, Kaiqiang Yu, Reynold Cheng, Laks V. S. Lakshmanan, and Xuemin Lin. 2019. Efficient Algorithms for Densest Subgraph Discovery. *Proc. VLDB Endow.* 12, 11 (2019), 1719–1732.

[12] Wassily Hoeffding. 1994. Probability inequalities for sums of bounded random variables. In *The collected works of Wassily Hoeffding*. Springer, 409–426.

[13] Shweta Jain and C. Seshadhri. 2017. A Fast and Provable Method for Estimating Clique Counts Using Turán's Theorem. In *WWW*.

[14] Shweta Jain and C. Seshadhri. 2020. The Power of Pivoting for Exact Clique Counting. In *WSDM*.

[15] Shweta Jain and C. Seshadhri. 2020. Provably and Efficiently Approximating Near-cliques using the Turán Shadow: PEANUTS. In *WWW*.

[16] Madhav Jha, C. Seshadhri, and Ali Pinar. 2015. Path Sampling: A Fast and Provable Method for Estimating 4-Vertex Subgraph Counts. In *WWW*.

[17] Jinyan Li, Guimei Liu, Haiquan Li, and Limsoon Wong. 2007. Maximal Biclique Subgraphs and Closed Pattern Pairs of the Adjacency Matrix: A One-to-One Correspondence and Mining Algorithms. *IEEE Trans. Knowl. Data Eng.* 19, 12 (2007), 1625–1637.

[18] Ronghua Li, Sen Gao, Lu Qin, Guoren Wang, Weihua Yang, and Jeffrey Xu Yu. 2020. Ordering Heuristics for k-clique Listing. *Proc. VLDB Endow.* 13, 11 (2020), 2536–2548.

[19] Rundong Li, Pinghui Wang, Peng Jia, Xiangliang Zhang, Junzhou Zhao, Jing Tao, Ye Yuan, and Xiaohong Guan. 2021. Approximately Counting Butterflies in Large Bipartite Graph Streams. *IEEE Transactions on Knowledge and Data Engineering* (2021), 1–1.

[20] Boge Liu, Long Yuan, Xuemin Lin, Lu Qin, Wenjie Zhang, and Jingren Zhou. 2020. Efficient (α, β)-core computation in bipartite graphs. *VLDB J.* 29, 5 (2020), 1075–1099.

[21] R. Milo, S. Shen-Orr, S. Itzkovitz, N. Kashtan, D Chklovskii, and U. Alon. 2010. Network Motifs: Simple Building Blocks of Complex Networks. *Science* 298, 5594 (2010), 763–764.

[22] Michael Mitzenmacher, Jakub Pachocki, Richard Peng, Charalampos E. Tsourakakis, and Shen Chen Xu. 2015. Scalable Large Near-Clique Detection in Large-Scale Networks via Sampling. In *SIGKDD, 2015*.

[23] Caixia Qin, Mingxue Liao, Yuanyuan Liang, and Changwen Zheng. 2019. Efficient Algorithm for Maximal Biclique Enumeration on Bipartite Graphs. In *ICNC-FSKD*.

[24] Mahmudur Rahman, Mansurul Alam Bhuiyan, and Mohammad Al Hasan. 2014. Graft: An Efficient Graphlet Counting Method for Large Graph Analysis. *IEEE Trans. Knowl. Data Eng.* 26, 10 (2014), 2466–2478.

[25] Seyed-Vahid Sanei-Mehri, Ahmet Erdem Sariyüce, and Srikanta Tirthapura. 2018. Butterfly Counting in Bipartite Networks. In *KDD*.
[26] Aida Sheshbolouki and M. Tamer Özsu. 2022. sGrapp: Butterfly Approximation in Streaming Graphs. *ACM Trans. Knowl. Discov. Data* 16, 4 (2022), 76:1–76:43.
[27] Bintao Sun, Maximilien Danisch, T.-H. Hubert Chan, and Mauro Sozio. 2020. KClist++: A Simple Algorithm for Finding k-Clique Densest Subgraphs in Large Graphs. *Proc. VLDB Endow.* 13, 10 (2020), 1628–1640.
[28] Etsuji Tomita, Akira Tanaka, and Haruhisa Takahashi. 2006. The worst-case time complexity for generating all maximal cliques and computational experiments. *Theor. Comput. Sci.* 363, 1 (2006), 28–42.
[29] Charalampos E. Tsourakakis. 2015. The K-clique Densest Subgraph Problem. In *WWW*.
[30] Jia Wang, Ada Wai-Chee Fu, and James Cheng. 2014. Rectangle Counting in Large Bipartite Graphs. In *IEEE International Congress on Big Data*.
[31] Kai Wang, Xuemin Lin, Lu Qin, Wenjie Zhang, and Ying Zhang. 2019. Vertex Priority Based Butterfly Counting for Large-scale Bipartite Networks. *Proc. VLDB Endow.* 12, 10 (2019), 1139–1152.
[32] Pinghui Wang, Junzhou Zhao, Xiangliang Zhang, Zhenguo Li, Jiefeng Cheng, John C. S. Lui, Don Towsley, Jing Tao, and Xiaohong Guan. 2018. MOSS-5: A Fast Method of Approximating Counts of 5-Node Graphlets in Large Graphs. *IEEE Trans. Knowl. Data Eng.* 30, 1 (2018), 73–86.
[33] Jianye Yang, Yun Peng, and Wenjie Zhang. 2021. (p, q)-biclique Counting and Enumeration for Large Sparse Bipartite Graphs. *Proc. VLDB Endow.* 15, 2 (2021), 141–153.
[34] Yixing Yang, Yixiang Fang, Maria E. Orlowska, Wenjie Zhang, and Xuemin Lin. 2021. Efficient Bi-triangle Counting for Large Bipartite Networks. *Proc. VLDB Endow.* 14, 6 (2021), 984–996.
[35] Xiaowei Ye, Rong-Hua Li, Qiangqiang Dai, Hongzhi Chen, and Guoren Wang. 2022. Lightning Fast and Space Efficient k-clique Counting. In *WWW*.
[36] Hao Yin, Austin R. Benson, and Jure Leskovec. 2017. Higher-order clustering in networks. *Physical Review E* 97, 5 (2017), 052306.
[37] Hao Yin, Austin R. Benson, Jure Leskovec, and David F. Gleich. 2017. Local Higher-Order Graph Clustering. In *KDD*.
[38] Yun Zhang, Charles A. Phillips, Gary L. Rogers, Erich J. Baker, Elissa J. Chesler, and Michael A. Langston. 2014. On finding bicliques in bipartite graphs: a novel algorithm and its application to the integration of diverse biological data types. *BMC Bioinform.* 15 (2014), 110.
[39] Yun Zhang, Charles A. Phillips, Gary L. Rogers, Erich J. Baker, Elissa J. Chesler, and Michael A. Langston. 2014. On finding bicliques in bipartite graphs: a novel algorithm and its application to the integration of diverse biological data types. *BMC Bioinform.* 15 (2014), 110.
[40] Alexander Zhou, Yue Wang, and Lei Chen. 2021. Butterfly Counting on Uncertain Bipartite Networks. *Proc. VLDB Endow.* 15, 2 (2021), 211–223.